Engineering homoaromatic substrate specificity into aliphatic-specific *Geobacillus pallidus* RAPc8 Nitrile Hydratase

Parikshant Kowlessur

A thesis submitted in partial fulfillment of the requirements for the degree of Magister Scientae in the Department of Biotechnology, University of the Western Cape.

Supervisor: Prof D.A Cowan

November 2007

Abstract

Engineering homoaromatic substrate specificity into aliphatic-specific *Geobacillus pallidus* RAPc8 Nitrile Hydratase.

Parik Kowlessur

Masters thesis, Department of Biotechnology, University of the Western Cape

Geobacillus pallidus RAPc8 is a thermophilic nitrile-degrading isolate, obtained from thermal sediment samples of a New Zealand hot spring. The *G. pallidus* RAPc8 NHase gene has been cloned and expressed in *E. coli*. The recombinant NHase exhibits nitrile-degrading activity at 50 °C, capable of degrading branched, linear and cyclic heteroaromatic nitrile substrates. However, no activity was found on homoaromatic nitrile substrates such as benzonitrile. In the present study, high levels of activity on benzonitrile were detected with a double mutant βF52GβF55L. Kinetic analysis on the mutant enzyme showed an 8-fold decrease in K_M with benzonitrile (0.3mM) compared to acrylonitrile (2.6mM). Specificity constants (k_{cat}/K_M) of 5900 and 450 $s^{-1}.mM^{-1}$ were obtained for the double mutant on benzonitrile and acrylonitrile respectively. The amino acid residues lining the substrate channel were identified and the geometric dimensions measured. Cavity calculations revealed a 29% increase in volume and a 13% increase in inner surface area for the substrate channel of the double mutant when compared to the wild type. Surface representation of the wild type structure revealed two extended, curved channels, which are accessible to the bulk solvent from two locations in the heterodimer. The removal of the βF52 may have contributed to the presence of a single channel with two opposing openings across the dimers with no internal blockage. Normal Mode Analysis calculations also indicate a higher intrinsic flexibility of the mutant relative to

the wild type enzyme. The increased flexibility within the mutant NHase could have introduced a functionally relevant aromatic substrate recognition conformation.

November 2007

Declaration

I declare that *Engineering homoaromatic substrate specificity into Geobacillus pallidus RAPc8 Nitrile Hydratase* is my own work, that it has not been submitted before for any degree or examination in any other university, and that all the sources I have used or quoted have been indicated and acknowledged as complete references.

Parik Kowlessur November 2007

Signed……

Acknowledgements

I would like to thank my supervisor, Professor Don Cowan for providing me with the opportunity to undertake this research in his laboratory. I would also like to thank my co-supervisor, Dr Muhammed Sayed. I gratefully acknowledged the invaluable help and advice of Professor Mike Danson from the University of Bath towards the successful completion of this work. It was such an honor to be taught by all of them.

A special thank to Sam Kwofie for his immense contribution towards the designing of the double mutant.

Many thanks to the Nitrile Hydratase group: Jennifer Van Wyk and Andrew Nel for their support and assistance in the lab.

I would like to thank Dr Heide Goodman for her kindness and motivation. I also thank Babele Emedi, Marshall Keyster, Walter Sanyika and Wycliff Musingarimi at the *Institute for Microbial Biotechnology and Metagenomics* for their sincere friendship.

I am most grateful to my parents for their love and continued support towards the completion of this thesis.

I gratefully acknowledged the National Research Foundation (SA) and the Royal Society of London (UK) for financially supporting this project.

Finally, I am thankful to the Lord God for giving me the strength and courage to make it all the way through.

Table of Contents

List of Tables

UNIVERSITY of the
WESTERN CAPE

List of Figures

Chapter 1: Literature Review

1.1 Introduction

Microbial degradation of nitrile compounds proceeds through two distinct enzymatic pathways. The first route involves the direct catalytic conversion of nitrile to their corresponding carboxylic acid moieties by the enzyme nitrilase (NTase; E.C 3.5.5.1) (Kato *et al*., 1998). The second is a bi-catalytic conversion of nitriles to the corresponding amides through the nitrile hydratase pathway (NHase; E.C 4.2.1.84) followed by a subsequent degradation to carboxylic acids by amidase (E.C 3.5.1.4) (Asano *et al*., 1982).

The study of nitrile-degrading enzymes, in particular NHase, has gained significant interest among many chemical manufacturers as it plays a key role in the synthesis of important commodity chemicals such as acrylamide and nicotinamide (Yamada and Kobayashi, 1996). However, despite its important commercial use, the *in vivo* physiological function of NHase remains obscure. It has long been presumed that the role of nitrile hydratase was linked to nitrogen detoxification within microbial strains (Legras *et al*., 1990). This hypothesis was recently rejected with the discovery of the aldoxime metabolizing pathway in certain microorganisms (Figure1); where aldoxime is degraded via a nitrile to the corresponding carboxylic acid by a combination of aldoxime dehydratase and nitrile hydrolyzing enzymes (Kato *et al*., 2004).

The pioneering research on the isolation of NHase from *Rhodococcus rhodochrous* J1 (Asano *et al*., 1980) has led to the identification of a large number of NHases in various microorganisms from diversified ecosystems including deep-sea hydrothermal vents (Heald *et al*., 2001), nitrile-contaminated soils (Padmakumar and

Oriel, 1999) and thermal lake sediments (Pereira *et al*., 1998). Despite this diversity in origin, many of the known NHase producing microorganisms belong to the genus *Rhodococcus*, although recently a number of NHases from thermophilic *Bacillus* species have been partially characterized (Tagashima *et al*., 1998; Padmakumar and Oriel, 1999). To date, no NHase have been identified in extremely thermophilic or hyperthermophilic microorganisms.

Enzyme characterization together with structure determination has led to the understanding of the biology, structure and mechanism of the metal containing nitrile hydratases. As a result, novel nitrile metabolizing microorganisms are continuously being exploited in search of thermostable NHases, which could have potential application as biocatalysts in industrial biotransformation. This chapter highlights the recent literature on NHases with particular emphasis on the molecular biology of the enzymes and their applications.

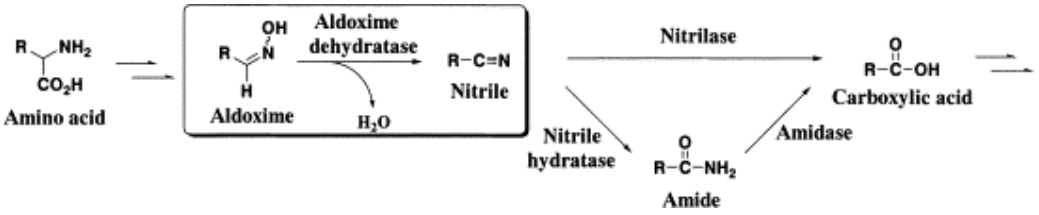

Figure 1.1: Aldoxime-nitrile pathway in microorganisms

1.2 Screening strategies for NHase-encoding genes

The isolation of nitrile-metabolizing organisms has largely been achieved using 'classic' trophic selection strategies where nitriles are offered as the sole source of carbon and/or nitrogen in order to favor growth of 'nitrilase' positive organisms

(Cowan *et al*., 2003). Although this method has proved to be highly successful, it limits access to the true extent of genomic diversity (Cunnigham *et al*., 1995; Pace, 1997). In reality, the standard microbiological method favors fast growing aerobic species (Schloss and Handelsman, 2003).

Prokaryotes represent by far the largest reservoir of genetic diversity on earth (Valera, 2004). Unfortunately, current estimates indicate that more than 99% of the microorganisms present in many natural environments are not readily culturable, thus leaving the overwhelming genetic and biological pool unexplored and unexploited (Streit and Schmitz, 2004). Therefore, an alternative approach to conventional enzyme screening is to access the wealth of genetic information through environmental nucleic acid extraction, avoiding the bottleneck of culture dependent methods (Cowan *et al*., 2005). Routine molecular biological techniques can then be applied to the community DNA preparations for molecular characterization of any target molecule.

This approach has been recently used to develop a molecular screening protocol based on PCR amplification to detect NHase-encoding genes (Laurenco *et al*., 2004). NHase sequences were retrieved from databases, aligned, after which primers were designed based on highly conserved motifs within the coding region of the NHase gene. This approach has been used to target NHase genes in various environmental samples (Precigou *et al*., 2001), where full-length NHase gene sequences were successfully amplified, cloned, and expressed in *E.coli*. However, it should be stressed that this particular method is not sequence independent as prior

knowledge of NHase sequences is required for effective primer design, and it is likely that the results are strongly biased toward the known NHase- producing groups.

1.3 Characteristic features of nitrile hydratases

1.3.1 Subunit structure and cofactor

NHases typically exist as heteromultimer complexes composed of two distinct α and β subunits with the basic stoichiometry of $\alpha_2\beta_2$ and M (M, Fe^{3+}or Co^{3+}) (Endo and Odaka, 2000). The two subunits range from 22 to 28 KDa and by convention the β subunit is found to be the largest. Their primary sequences are well conserved, but there is no apparent homology between the two subunits (Miyanaga *et al*., 2001). So far, all known NHases are found to be functional only as tetramers (Huang *et al*., 1997). The static structure of the enzyme shows that the tetramer exists as an asymmetric unit consisting of two dimers (Miyanaga *et al*., 2001). Early studies suggested that NHases from *Rhodococcus* sp. R312 required a pyrroloquinoline quinone (PQQ) cofactor (Yamada and Kobayashi, 1996). The role of the (PQQ) cofactor was attributed to a biological oxidation-reduction mechanism participating in the hydration of the nitrile group (Nagasawa and Yamada, 1989). However, this hypothesis was ultimately rejected with the resolution of the enzyme's crystal structure (Huang *et al*., 1997) where no PQQ cofactor was identified. To date, crystal structures as well as numerous spectroscopic studies reveal that NHases either contain a low- spin non-haem Fe (III) ion per α β dimer, or a non-corrinoid Co (III) ion per αβ dimer (Miyanaga *et al*., 2001). NHases are thus characterized as Fe- type or Co-type. The Co-type NHases appear to display broader substrate specificity (capable of hydrating a wider range of nitrile compounds) and higher molecular

stability than the Fe-type counterparts. All thermophilic NHases belong to the Co-type group.

1.3.2 Photoactivation

The activity of NHases from several *Rhodococcus* species exhibits unique features when exposed to light (Kobayashi and Shimuzu, 1998). In particular, activity in the NHase from *Rhodococcus* sp. N771, the best characterized of all the iron containing NHase family (Endo *et al*., 2001), is lost during aerobic incubation in the dark but almost completely recovered upon light irradiation (Endo and Odaka, 2000). This phenomenon is intrinsic to the enzyme even though the photoactivated NHase cannot be inactivated by darkness *in vitro*.

The overall mechanism was assessed using difference Fourier-Transform Infra-Red (FT-IR) spectra measured before and after photoreactivation of NHase (Nogushi *et al*., 1995). Spectroscopic analysis indicated that nitrile hydratase was reversibly inactivated in the dark due to the binding of an endogenous nitric oxide molecule to the iron (Mascharak, 2002). The enzyme activity was restored by photo-irradiation suggesting a structural change at the iron centre, leading to the subsequent breakage of the Fe-N bond (Endo *et al*., 1999). Similar results in *Rhodococcus* sp. N774 and R312 were also reported (Endo and Odaka, 2000). The mechanism of photoreactivation and dark inactivation is illustrated schematically in Figure 1.2. It has been demonstrated that Fe-type NHase from *Comamona testosteroni* N11 that only shares 50 % sequence homology with N771 (Artaud *et al*., 1999) and is insensitive to light *in vivo* also displays photoreactivity in the presence of exogenous nitric oxide

(Stevens *et al*., 2003). This suggests that the binding and photodissociation of nitric oxide may be a common phenomenon to all iron-type NHase.

Nevertheless, the origin of the nitric oxide within the microorganisms still remains unclear. It was proposed that a nitric oxide synthetase activity could possibly be responsible for the catalytic conversion of L-arginine into L-citrulline and nitric oxide in *Rhodococcus* sp. R312 (Sari *et al*., 1998)). However, crude extracts from *Rhodococcus* sp. N771 showed no activity for the conversion of (^{14}C) L-arginine into (^{14}C) L-citrulline (Artaud *et al*., 1999). Therefore, although the nitric oxide producing system in the microorganisms is still uncertain, this mechanism might have potential applications in the designing of novel photoreactive chemical compounds or proteins involved in the use of biochips and light controlled metabolic systems (Endo *et al*., 1999).

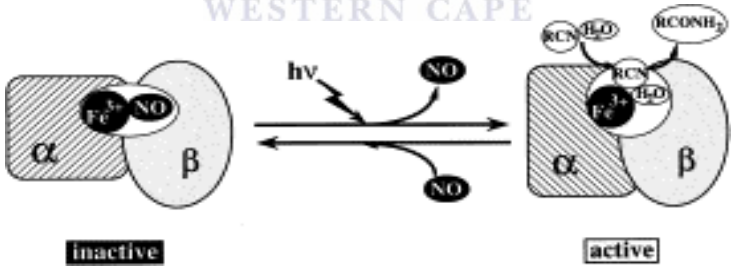

Figure 1.2: Schematic diagram of the regulation of the photoreactive NHase from *Rhodococcus* sp. N771 by nitrile oxide

1.3.3 Substrate specificity

Many NHases characterized so far display higher levels of substrate specificity (k_{cat}/K_M) for aliphatic nitriles over aromatic ones. However, some enzymes with activity on aromatic nitriles have also been described. It was first claimed that the

iron-containing NHases family was better suited for hydration of aliphatic nitriles whereas the cobalt containing-ones were specific for aromatic nitriles (Kobayashi and Shimuzu, 1998). This hypothesis could no longer be supported with the characterization of the Fe-type NHase of *Rhodococcus erythropolis* that exhibits broad substrate specificity capable of hydrating aliphatic, aromatic as well as heterocyclic nitrile compounds (Duran *et al*., 1993). The cobalt type enzymes of *Bacillus smithii* (Tagashima *et al*., 1998), *Bacillus pallidus* Dac 521 (Cowan *et al*., 1998) and *(Geo) Bacillus* RAPc8 (Pereira *et al*., 1998) do not show any activity on aromatic nitriles (Table 1.1).

The crystal structure of the nitrile hydratase (NHase) from *Bacillus smithii* SC-J05-1 shows that the β-subunit contains phenylalanine (Phe 52) which covers the metal centre partially like a small lid, narrowing the active site cleft, thus enabling only small aliphatic molecules to enter the catalytic site (Hourai *et al*., 2003).

Several NHases with very broad specificity profiles have been described as well (Table 1.2). The characterization of NHase from *Rhodococcus erythropolis* BL1 shows that it has wide substrate specificity; aliphatic nitriles such as butyronitrile and aromatic nitriles such as benzonitrile were good substrates (Duran *et al*., 1993). Similarly, *(Geo) Bacillus* sp. RAPc8 demonstrated activity on a wide range of aliphatic substrates including branched, linear, cyclic-aliphatic and di-nitriles but failed to catalyse homoaromatic nitriles such as benzonitrile (Pereira *et al*., 1998). The L-NHase and H-NHase of *Rhodococcus rhodochrous* J1 preferentially degrade aromatic nitriles (Kobayashi *et al*., 1992). However, the affinity and activity of L-NHase for aromatic substrates was found to be significantly higher than that of H-

NHase (Wieser *et al*., 1998). Although a few known nitrile hydratases are capable of hydrating both aromatic and aliphatic nitriles with high k_{cat} values, the remaining NHases can only show high levels of substrate specificity (k_{cat}/K_M) on either aliphatic or aromatic nitriles but not both (Yamada and Kobayashi, 1996). It has been suggested that such conclusions should be reassessed, as some potential substrates may also act as potent competitive inhibitors (Cramp and Cowan, 1999).

Some NHases have also been reported to display enantioselectivity. For instance, *Agrobacterium tumefaciens* d3 NHase showed enantioselectivity from a number of racemic phenylpropionitriles. *P. putida* NHase was also found to produce (S)-amides through the conversion of a racemic mixture of 2-(4-chlorophenyl)-3-methylbutyronitrile (Fallon *et al*., 1997).

Table 1.1: Substrate specificities of various NHase producing microorganisms

Organism	Metal Cofactor	Substrate specificity	Reference
Thermophilic			
(Geo) Bacillus sp. RAPc8	Co	Very wide: cyclic, linear, dinitriles and branched aliphatic	Pereira *et al*., 1998
Bacillus pallidus DAC521	Co	Narrow: aliphatic	Cowan *et al*., 1998
Bacillus smithii SC-J05-1	Co	Wide: linear, aliphatic, branched aliphatic and dinitriles	Takashima *et al*., 1998
Mesophilic			
Corynebacterium sp. C5	Fe	Narrow: aliphatic	Yamamoto *et al*., 1992
Rhodococcus sp. R312	Fe	Wide: aliphatic, cyclic	Nagasawa *et al*., 1986

Table 1.2: Comparison of substrate specificities of various bacterial NHases.

Substrate	[1]***(Geo) Bacillus pallidus* RAPc8**	[2]***Bacillus pallidus* DAC521**	[3]***Bacillus smithii***	[4]***Rhodococcus erythropolis***
Acetonitrile	100	28	540	5
Chloroacetonitrile	43	-	-	20
Acrylonitrile	67	37	390	45
Propionitrile	32	19	100	15
butyronitrile	46	26	290	100
Valeronitrile	108	23	240	-
cis, trans crotonitrile	50	38	23	-
Benzyl cyanide	0	-	-	-
Benzonitrile	0	0	1	46
3-Cyanopyridine	53	-	4	55

Values are relative activities (%, ±5 %). Data from: [1] Pereira *et al*. (1998), [2] Cameron (2002), [3] Cramp (1998) and [4] Duran *et al*. (1993)

1.3.4 Reaction Mechanisms

The mechanism for the hydrolysis of nitriles by NHases still remains unclear. To date, three plausible mechanisms have been suggested (Figure 3) (Nelson *et al*., 1991).

a) A hydroxide ligand from the coordination sphere of the metal centre is displaced by the nitrile substrate. A water molecule then hydrolyses the

metal-substrate complex, giving rise to a metal bound imminol intermediate. Ultimately, the intermediate rearranges to the amide product before releasing the amide.

b) The nitrile carbon is subjected to nucleophilic attack by metal bound hydroxide ion. The reaction generates a transient imminolate species that rearranges into an amide.

c) The metal bound hydroxide causes deprotonation of a free water molecule near the active site. The newly generated hydroxide carries out the nitrile substrate hydrolysis.

The third mechanism does not involve ligand exchange (Huang *et al*., 1997). The similarity in conversion rates with both Fe- and Co NHases under the same reaction conditions makes mechanism 3 to be the most plausible model (Mascharak, 2002).

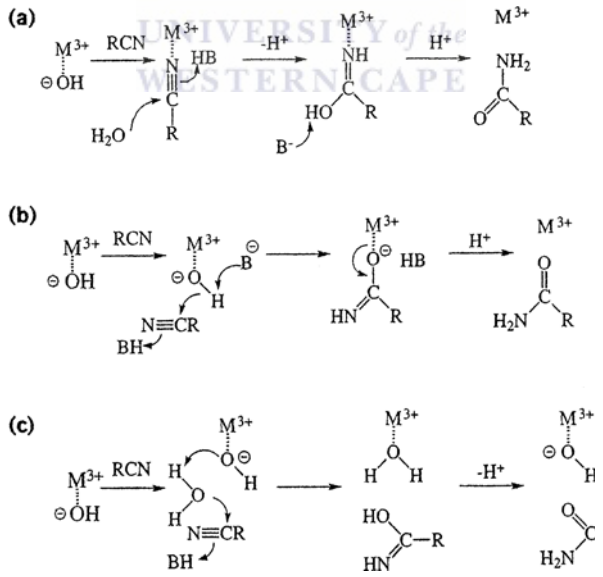

Figure 1.3: Possible mechanisms of nitrile hydration

1.4 Structural differences between Fe-type and Co-type NHases

1.4.1 Fe-type NHases

The structure of the Fe-type NHase from *Rhodococcus* sp. R312 has been the most studied of all known NHases (Huang *et al*., 1997). Early spectroscopic studies described the active site as a six coordinate, low spin Fe^{3+} ion with single oxygen, two sulfur and three nitrogen ligands (Nelson *et al*., 1991). The nitrogen ligands were attributed to the imidazole nitrogen of the histidine residue whereas the oxygen was thought to belong to a hydroxide ion (Kobayashi and Shimuzu, 1998).

These data have been reevaluated following crystallographic analysis of *Rhodococcus* sp. R312 NHase, an enzyme that has 100% sequence homology with *Rhodococcus* N771 NHase (Artaud *et al*., 1999). The X-ray structures, solved at a resolution of 2.65 Å and 1.7 Å, revealed a unique structure of the ferric NHase for the photoactivated *Rhodococcus* sp. R312 NHase (Huang *et al*., 1997) and nitrosylated *Rhodococcus* sp. N771 NHase (Nagashima *et al*., 1998), respectively. In both cases the two structures were very similar, suggesting that the conformation was conserved between active and inactive states. In each case, the crystallographic asymmetric unit was made up of two αβ heterodimers. The α-subunit contained of a long N-terminal arm and a C-terminal domain that formed a novel fold (Mascharak, 2002). This fold had a four layered structure αββα, with unusual connections between the β strands. The β chain started with a long loop of 30 residues that wrapped around the α-subunit in the dimer. It also contained a long N-terminal extension, a helical domain and a C-terminal domain that folded into a β roll (Endo *et al*., 1999). The two subunits formed a tightly bound heterodimer with a novel iron centre located in the interior of a

large open cavity at the subunit-subunit interface. The iron centre was composed of four sulphur atoms from three cysteine residues and two main-chain amide nitrogen atoms. The five ligands were positioned at five vertices of an octahedron, the sixth site of which remained unoccupied in the crystal structure (Mascharak, 2002). Therefore this new conformation does not comply with the two sulfur, three nitrogen and oxygen prediction (Nelson *et al*., 1991) as no histidine residues were found within the cavity. The nitric oxide occupied the sixth coordination site, which was accessible from the solvent and was thought to be the catalytic site (Endo and Odaka, 2000). This result supports the previous findings that direct binding of nitric oxide to the non-haem iron centre causes the inactivation of NHases (Huang *et al*., 1997).

Mass spectrometry on a tryptic peptide photoactivated enzyme revealed that the α-cysteine 112 from *Rhodococcus* sp. N771 was post-translationally modified to a cysteine sulfinic acid (Cys-SO_2H). Furthermore, the crystal structure demonstrated that α-cysteine 114 was also post-translationally modified to a cysteine sulfenic acid (Cys-SOH) (Nagashima *et al*., 1998). Despite having an identical amino acid sequence and photoreactive behavior, the crystal structure of *Rhodococcus* sp. R312 NHase did not display such modifications. A proposed mechanism was thus established where the nitric oxide molecule was thought to be stabilized by the oxygen atoms of three cysteine molecules that protruded from the plane containing the iron centre, like claws. This previously unreported structure is termed ‘claw setting’ (Figure 1.4). Light irradiation not only breaks the Fe-N bond but also induces a structural change in the claw setting that weakens the interaction between the oxygen atoms and nitric oxide (Nagashima *et al*., 1998). The α-cysteine 113 and α-

cysteine 115 form hydrogen bonds with β-arginine 56 and β-arginine 141, which are conserved through all known NHases (Huang *et al*., 1997). Mutations of these residues resulted in loss of enzymatic activity, suggesting that they are involved in the stability of the claw setting, which in turn is crucial for the NHase activity. The 10 Å wide entrance of the inactive N-771 enzyme is too narrow for substrates to enter (Nagashima *et al*., 1998). It is therefore thought that dynamic structural changes brought about during light activation are required to open the channel, which leads to the active centre during the catalytic cycle.

1.4.2 Co-type NHases

Until recently, little structural information was available on cobalt-type NHases. The crystal structure of a cobalt-type NHase from *P. thermophilia* was only recently determined at a resolution of 1.8 Å (Miyanaga *et al*., 2001). The structure revealed a non-corrinoid cobalt at the catalytic centre coordinated with two cysteine residues (α-Cys 111 and α-Cys 113). The two residues were both post-translationally modified to cysteine sulfinic acid and to cysteine sulfenic acid, respectively, giving rise to a similar claw setting as in iron containing nitrile hydratases. However, replacement of a tryptophan residue by a tyrosine residue was noted at the catalytic site; such a structural change could possibly account for the differences in substrate selectivity. The -V-C- (T/S)-L-C-S-C- sequence that forms a highly conserved protein motif among all NHases has a diagnostic threonine residue in the third position for the cobalt nitrile hydratase and a serine residue for the iron nitrile hydratase (Kobayashi and Shimuzu, 2000).

The Fe-type and the cobalt type NHases display high structural similarity in the α subunits only. However, a major structural difference is noted in the β subunits. In particular, residues between β 95 and β 138 of the Co-NHase show little homology when compared to the Fe-type NHase (Miyanaga *et al*., 2001). On alignment of the central portion of this region, an insertion of 12-25 residues was noted in the cobalt-type NHase. In addition, the *P*. *thermophilia* NHase structure revealed that this region gave rise to an α-helix, which interacted with a second α helix on the external surface of the α-subunit. It has been suggested that this additional interaction may contribute towards the thermostability of the enzyme (Miyanaga *et al*., 2001). However, similar sequences are also found in the Co-type NHases of *Rhodococcus* sp. and *R. rhodochrous* J1, neither of which are particularly thermostable enzymes (Kobayashi and Shimuzu, 1998).

It has been reported that substitution of the iron cofactor with cobalt ions in *Rhodococcus* sp. N771 NHase had absolutely no effect on the enzymatic activity of the enzyme (Endo *et al*., 2001). This study supports the hypothesis that Co and Fe-type NHase share very similar structures and presumably, reaction mechanisms.

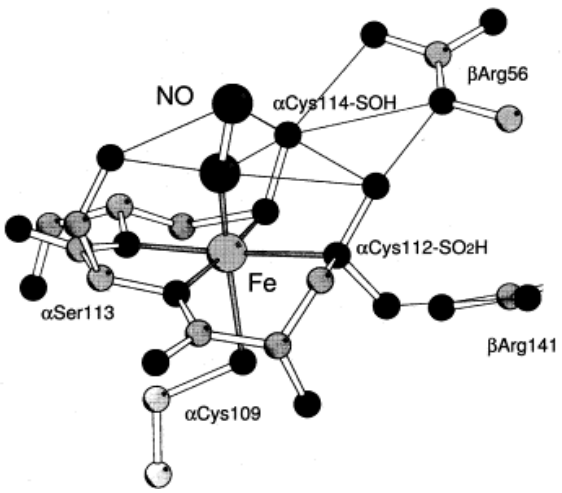

Figure 1.4: The 'claw setting' of nitrile hydratase

1.5 Molecular biology of NHases

1.5.1 NHase operon

The genes for various nitriles–modifying enzymes had successfully been cloned using a wide array of techniques. One of the conventional approaches had been the determination of the N-terminal and internal amino acid sequences of the proteins from which oligonucleotides were designed either for use as probes or to produce PCR products (Kobayashi *et al*., 1992). For instance, N774 NHase genes had been extensively used as probes in the Southern blot technique for the isolation of *R. rhodochrous* and *R*. *erythropolis* NHase genes (Duran *et al*., 1993). In addition, PCR primers designed against multi-sequence alignment of NHase genes of *Rhodococcus* from different gene banks had been used for the isolation of the corresponding genes of *Nocardia* sp. using the PCR technique (Shi *et al*., 2004).

Northern blot analysis using RNA as probes revealed that the NHase gene is arranged within a gene cluster on an operon (Bigey *et al*., 1999). The size of the α subunit gene was estimated to be in the range of 609 to 660 bp while the β subunit gene consisted about 636 to 706 bp. The distance separating the two subunits was approximately 25 bp and their arrangement on the operon varies from species to species (Kim and Oriel, 2000). The cloned *Rhodococcus* sp. N-774 NHase gene showed adjacent subunits arrangement with the α preceding the β (Ikehata *et al*., 1989). With the exception of the H-NHase operon of *Rhodococcus rhodochrous* J1, all the NHase genes described so far are positioned approximately 100 bp downstream from an amidase gene (Duran *et al*., 1993). Transcription terminators characterized by stabilized stem loop structures were also identified downstream of

the nitrile operon. The absence of such terminators between the amidase and the NHase suggests the co-expression of both genes as a single polycistronic mRNA (Bigey *et al*., 1999). Certain NHase producing microorganisms require an activator protein that normally flanks the NHase genes for overexpression of active NHase. Overproduction of *Geobacillus* sp. RAPc8 NHase requires co-expression of P14K, a 14-Kda protein downstream of the β-subunit (Cameron, 2002). Arrangement of the gene clusters from various NHase producing organisms is shown in Figure 1.5.

The NHases also revealed significant consistencies in their structure and organization at the amino-acids level. The cysteine cluster regions (CXCC) coordinating with the iron or cobalt cofactors at the catalytic site cleft is fully conserved (Hashimoto *et al*., 2002). Site directed mutagenesis performed in this highly conserved cysteine rich motif (CXCC) by substituting each of the cysteine residues with a serine residue lowered the expression efficiency of active NHase considerably (Lu *et al*., 2003). Their presence in fact enhanced active over-expression. The –VC (T/S) LCSCY- cofactor binding motif is also highly conserved in the α subunit of all known NHase producing microorganisms (Kobayashi and Shimuzu, 1998).

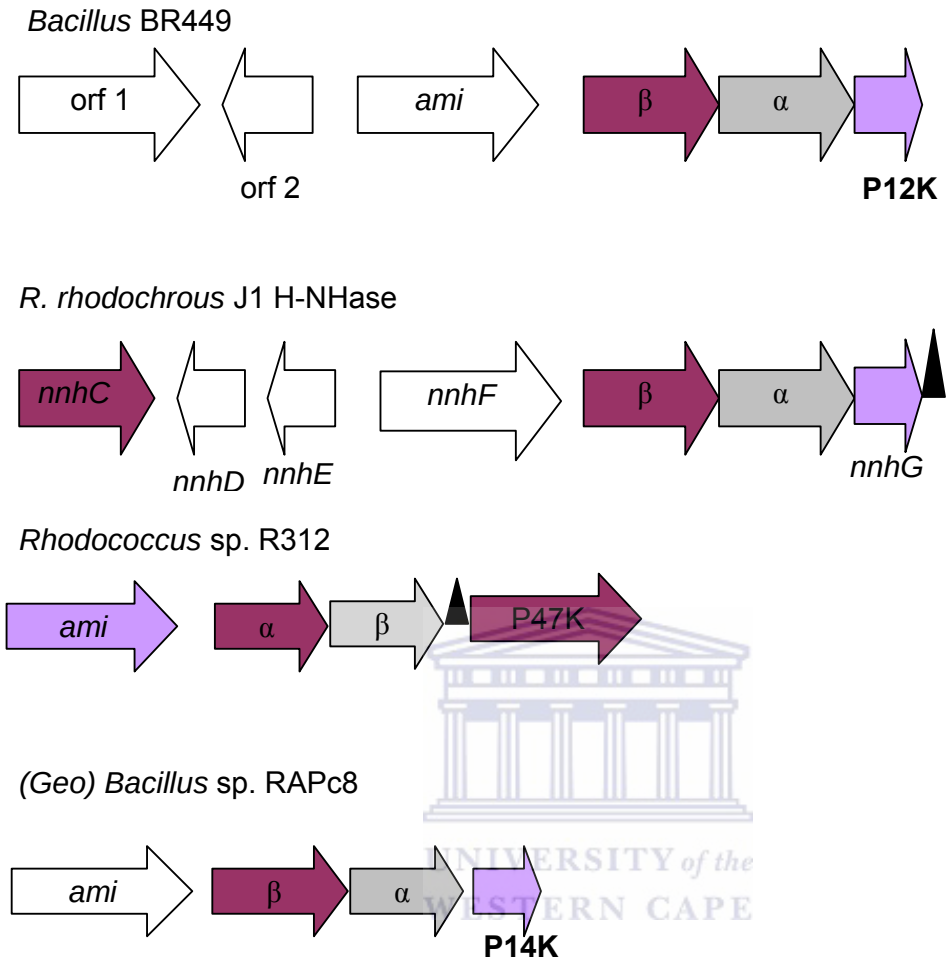

Figure 1.5: Gene clusters arrangement from various NHase producing organisms. Arrows indicate the direction and extent of the genes. Stem loop structures that serve as potential transcriptional terminators are shown as black triangles.

1.5.2 Functional expression of NHase

The requirements for functional expression of active NHase vary from organism to organism. Some NHases are expressed constitutively whilst others have shown to be inducible (Duran *et al*., 1993). In fact, various reports show that NHase is generally induced by their amides (reaction products) rather than by their nitriles (reaction substrates) (Kobayashi and Shimuzu, 1998). Whilst the literature contains no

information containing the effect of supplementing Fe^{2+} ions to the growth media of Fe-type NHase producers, experiments have shown that incubation of NHase apoenzyme with Co^{2+} ions enhanced greatly the activity of NHase. In fact, both BR449 (Kim and Oriel, 2000) and RAPc8 (Cameron *et al*., 2005) NHases are expressed as inactive apoenzyme when grown in the absence of cobalt ions. These findings perhaps suggest that cobalt is involved in enhancing protein activity rather than induction of NHase expression.

Early attempts at recombinant expression of active NHase were largely unsuccessful, and resulted in the production of insoluble and inactive inclusion bodies (Yamada and Kobayashi, 1996). This problem has ultimately been overcome with the discovery of the 'activator protein' (Kobayashi and Shimuzu, 1998). The co-expression of the 'activator protein' with NHase significantly enhanced active over-expression. In this regard, several NHase from various microorganisms have successfully been expressed as active enzymes in *E. coli* or *R. rhodochrous* strains in the presence of their respective activators (Lu *et al*., 2003). However, expression of NHase from a moderate thermophilic *Bacillus* sp. BR449 appeared to be unique in that the co-expression of the 'activator protein' gene seemed to have no effect on the NHase expression or activity (Kim and Oriel, 2000).

The mechanism by which these 'activator protein' assists in NHase expression remains unclear. However, there is a general belief that the activator may be necessary for incorporation of the metal ion into NHase. In addition, there could be a possibility that the activator might be involved in the post-translational modification of α Cys 112 and/or α Cys114 (Endo *et al*., 2000). Recently, modeling of a P14 K

protein structure derived from the moderate thermophilic *(Geo)Bacillus* sp. RAPc8 revealed that the latter may function as a molecular chaperone aiding in NHase folding resulting to the formation of (α_2 β_2) heterodimer (Cameron *et al*., 2005). Further studies on the role of these activators are still in progress.

1.6 Applications of NHases

1.6.1 Biotransformation

In the early 1980s, microbial catalysis using NHases emerged as an alternative to the classical chemical conversion of nitrile compounds (Zaks, 2001). Consequently, NHases became the catalyst of choice due to their unique method of hydrolysis. The enzymes are capable of hydrating a wide range of nitrile compounds due to their high regioselectivity and chemoselectivity properties. NHase can be a substitute to the harsh industrial chemical reaction conditions or high reaction temperatures (Thomas *et al*., 2002). In addition, NHases allow industrially driven processes to be less costly and thus commercially more desirable (Mylerova and Martinkova, 2003).

A successful NHase application is the industrial kiloton-scale production of acrylamide from acrylonitrile. The bulk synthesis of biologically synthesized acrylamide is due to its use as an ingredient in the production of various polymers (Yamada and Kobayashi, 1996). Acrylamide is commonly used in coagulators and soil conditioners, for paper treatment and paper sizing, and for adhesives, paints and petroleum recovery agents (Kobayashi *et al*., 1992). The conventional approach uses copper salts as a catalyst for the hydration of nitrile compounds (Nagasawa and Yamada, 1989). However, this method is associated with some drawbacks. In particular, the waste stream of this process contained toxic copper ions and

unreacted acrylonitrile, causing environmental pollution. Moreover, the disposal of the large amount of by-products including acrylic acid remaining in the reactor was very difficult. The enzyme production of acrylamide started in 1985 using *Rhodococcus* sp. N774 as the first generation strain isolated by Nitto Chemical Industry (Nagasawa and Yamada, 1989). Since then, intensive research was focussed on improving the nitrile hydratase activity. In 1988, the second-generation strain, *P. chlororaphis* B23, was introduced for the same purpose (Nagasawa and Yamada, 1989). In 1991, high NHase activity was discovered in *R. rhodochrous* J1.

The *R. rhodochrous* J1 NHases act not only on acrylonitrile, but also on other aliphatic as well as aromatic nitrile substrates (Nagasawa and Yamada, 1995). Nicotinamide (vitamin B_3), also generated by nitrile hydratase, is a vitamin generally used in animal feed supplementation (Yamada and Kobayashi, 1996). Lonza Guangzhou Fine Chemicals (China) began nicotinamide synthesis using a four-stage chemozymatic production. The starting material 3-methyl-1,5-diaminopentane (a nylon 6,6 by-product) is catalytically converted into 3-picoline, which in turn is ammoxidated to 3-cyanopyridine before being hydrolysed to nicotinamide (Thomas *et al*., 2002). However, this process was undesirable due to contamination by nicotinic acid, a reaction by-product (Nagasawa and Yamada, 1989). Therefore, besides its low energy usage, bioprocess produces the desired amide at a purity of over 99.3 % (Heveling *et al*., 1998; Shimuzu, 2001). The currently used bioprocess involves a four stage chemo-enzymatic synthesis using the nylon-6,6 byproduct, 2-methyl 1, 5-diaminopentane, as the starting material. The latter is catalytically converted into 3-picoline, which is subsequently ammoxidated into 3- cyanopyridine

before ultimately being hydrolyzed to nicotinamide using immobilized *R. rhodochrous* J1 cells (Thomas *et al*., 2002).

The use of cultured *R. rhodochrous* J1 cells in the presence of crotonamide also gives rise to a wide variety of useful amides with high productivity yield. For instance, isonicotinamide is used for the industrial production of isonicotinic acid hydrazide, which is a tuberculostatic. Moreover, 2, 6-difluorobenzamide is useful for the synthesis of agricultural chemicals (Yamada and Kobayashi, 1996).

A further example of a NHase catalyzed synthesis currently in use is the production of a Du Pont (USA) herbicide azafenidine from 5–cyanovaleramide (5-CVAM). Originally, 5-CVAM was produced from the chemical hydration of adiponitrile (ADV) using manganese dioxide as a catalyst. However, problems associated with low conversion rates (~ 25%) and significant production of the by-product adipamide (ADAM), solvent extraction and catalysts deactivation led to the development of a biocatalytic process (Thomas *et al*., 2002).

1.6.2 Bioremediation

Significant amounts of synthetic nitriles are spread in the environment, predominantly in the form of industrial wastewater (Kobayashi and Shimuzu, 1998). Various strategies have been adopted to reduce the destructive effect of these effluents. However, these methods were too costly. To date, two main approaches are recognized for remediation of acrylonitrile. The first method involves the enzymatic treatment of acrylonitrile in an aqueous polymer emulsions used in raw rubber and plastic manufacture (Battistel *et al*., 1997). The second viable approach makes use of

specialized consortia of microorganisms to degrade toxic wastes. A stable activated sludge system was developed whereby the bacteria containing nitrile-degrading enzymes that metabolize effluents were grown on the waste components resulting in complete degradation (Wyatt and Knowles, 1995).

Several nitrile herbicides are now used in agriculture: e.g., 2, 6 – dichlorobenzonitrile and bromoxynil (Kobayashi and Shimuzu, 1998). Even though they have proved to be highly effective, they are still considered as potential threat to the environment. As a result, NHase is probably the perfect candidate for the degradation of these toxic nitriles herbicides. Consequently, transgenic plants carrying the microbial bromoxynil-specific NHase gene have been designed. Tobacco or tomato transgenic plants, with a NHase gene within their genome could possibly be on the market in future (Stalker *et al*., 1988).

1.7 Aim and Objectives

The primary aim of this study is to continue work aimed at engineering homoaromatic substrate specificity in *Geobacillus pallidus* RAPc8 NHase by site directed mutagenesis. Structural analysis has shown a narrow substrate channel in the RAPc8 NHase, suggesting that larger molecules such as aromatic nitriles may not access the active site. The strategy used will aim to increase catalytic site volume by replacing bulky aromatic residues lining the substrate channel with smaller aliphatic ones. To achieve this aim the following objectives will be pursued:

1. *In silico* modeling for the designing of new mutants.
2. Expression and purification of the mutant

3. Kinetic analysis
4. Structural analysis

Chapter 2: Materials and Methods

2.1 Chemicals and reagents

Unless otherwise stated, Merck Chemicals and Laboratory supplies, Sigma Aldrich Chemical Company and Kimix Chemical and Laboratory Supplies supplied all chemicals of analytical/reagent grade.

DNA size markers, protein size markers and all DNA modifying enzymes (polymerises and restriction endonucleases) were purchased from Fermentas Life Sciences Ltd.

Integrated DNA Technologies (IDT) Inc synthesized all the oligonucleotide primers for polymerase chain reaction (PCR).

Oxoid Ltd and Biolabs supplied culture media

2.2 Bacterial strains

Table 2.1: The bacterial strains used in this study,

Bacterial strain	Relevant Genotype	Supplier
E. coli XL-1 Blue	RecA1 endA1 gyrA96thi-hsdR17 sup E44 re (A) lac [F^1 proAB $lacI^q$ ZM15 Tn10 (Tet^r)]	Stratagene
E. coli BL 21 (DE3)	*HsdS gal ompT* (λcIts857 *ind* 1 Sam7 *nin*5 lacUV-T7 gene1)	Stratagene
E. coli BL 21 pLysS	As above. (pLysS)	Stratagene

2.3 Plasmids

Table 2.2: Expression plasmids used throughout this study

Plasmid	Description	Source
pET21a (+)	High-level expression vector containing an ampicillin resistance gene	Novagen
pNH14K (also known as pNH461)	A derivative of the pET21a (+) carrying the α and β subunit genes together with the P14K gene of the *Geobacillus* pallidus RAPc8 NHase	Cameron *et al*., 2005
pNH14K βF55L	NHase βF55L mutant of pNH14K	Cameron, 2002
pNH14K βF52GβF55L	NHase βF55LβF2G mutant of pNH14K	Kwofie, 2006
pNH14K αY122G	NHase αY122G mutant of pNH14K	This work

2.4 Buffers and solutions

Table 2.3: Buffers and solutions

Buffer/Solution	Composition	pH
Agarose gel loading dye (6X)	0.25 % (w/v) bromophenol blue 40 % (w/v) sucrose	
Ammonia assay reagent A	0.59 M phenol 1 mM sodium nitroprusside	
Ammonia assay reagent B	0.11 M sodium hypochlorite 2 M sodium hydroxide	
1 M Potassium phosphate buffer	717 ml 1 M K_2HPO_4 283 ml 1 M KH_2PO_4	7.2
SDS-PAGE electrode buffer (10X)	0.25 M Tris HCL 2 M glycine 1 % SDS	8.3
SDS-PAGE Gel-loading buffer	100 mM Tris-Cl 4 % (w/v) SDS 0.2 % (w/v) bromophenol blue 20 % (v/v) glycerol 200 mM dithiothreitol	6.8
PAGE staining solution	0.2 % Coomasie Blue R 250 40 % methanol 10 % acetic acid	
PAGE destaining solution	40 % methanol 10 % acetic acid	
20 X TAE buffer	2 M Tris base 25 mM EDTA (pH adjusted with glacial acetic acid)	8.3

2.5 Analytical procedures

2.5.1 Spectrophotometry

Spectrophotometric analyses were performed using a Biomate 3 spectrophotometer (Thermo Electronic Company) or a Cary 300 *Bio* spectrophotometer operated via WinUV software (Varian Ltd).

2.5.2 Determination of protein concentration

Protein concentrations were determined using the Biorad Protein Assay, with BSA as the standard (Bradford, 1976). BSA concentration in the range of 0-1.4 mg/ml was used. A typical standard curve as shown in Appendix 1 was used to calculate the protein sample concentrations.

2.5.3 Polyacrylamide gel electrophoresis

Protein separation by SDS PAGE was performed using a Hoefer Slab unit SE 280. Ideally, 0.75 mm gels containing 12 % acrylamide were prepared using the Hoefer SE 245 dual gel caster. Protein samples (6 µl) were prepared by suspending in SDS PAGE gel loading buffer (2 µl) and brief boiled prior to loading (Sambrook and Russel, 2001). Protein samples were electrophoresed at a constant current of 15 mA. Following electrophoresis, gels were stained with Coomassie Blue, and then destained overnight using PAGE destaining solution.

Table 2.4: SDS PAGE (12 %) separating gel components.

Components	Volume (ml)
ddH_2O	6.6
1.5 M Tris-HCl, pH 8.8	5
20 % (w/v) SDS	0.2
30 % Acrylamide/0.8% Bis-acrylamide 0.8 % (w/v)	8
10 % (w/v) ammonium persulfate	0.2
TEMED	0.01

Table 2.5: SDS PAGE stacking gel components.

Components	Volume (ml)
dd H_2O	2.8
0.5 M Tris-HCl, pH 6.8	1.25
20 % (w/v) SDS	0.05
30 % Acrylamide/0.8% Bis-acrylamide 0.8 % (w/v)	0.85
10 % (w/v) ammonium persulfate	0.05
TEMED	0.005

2.5.4 NHase activity assays

The ammonia detection assay is a calorimetric assay, quantifying the release of ammonia using the modified phenol-hypochlorite detection method (Fawcett and Scott, 1960). The assay was carried out as described previously (Cramp and Cowan, 1999). When assaying recombinant NHase, the reaction mixture was supplemented with an excess of recombinant *G. pallidus* amidase. The blue product formed was detected spectrophotometrically at 600 nm absorbance and the results interpolated against a standard curve prepared using 0-2mM ammonium chloride. All assays were performed in duplicate.

2.5.5 Kinetic studies

A continuous spectrophotometric assay was used for all kinetic analyses. Assays were done in triplicate at 50 °C in quartz cuvettes. The reaction mixture consisted of 50 mM potassium phosphate buffer, pH 7.2, with 0-30mM acrylonitrile or 0-1mM benzonitrile dissolved in methanol to a final volume of 1 ml for the mutant enzyme. Reagents were equilibrated by incubation at 50 °C. Purified *G. pallidus* NHase (150 ng for acrylonitrile and 100 ng for benzonitrile) was added to initiate the reaction. Hydration of acrylonitrile and benzonitrile was monitored at 225 and 242 nm, respectively, on a Cary 300 *Bio* spectrophotometer operated *via* WinUV software (Varian Ltd). The molar extinction coefficients of acrylamide and benzamide are 2.9 and 5.5 mM^{-1}. cm^{-1}, respectively. All the kinetic data were analyzed using the program Enzpack (Biosoft). The direct-linear plot was the straight-line transformation graph of the Michaelis-Menten equation that was used for statistical analysis of the enzyme kinetic data (Eisenthal and Bowden, 1974). For enzyme inhibition studies, assays were repeated in the presence of 200μM benzonitrile.

2.6 Site-directed mutagenesis

The recombinant plasmid containing the β and α NHase subunits and P14 K activator gene cloned at the multiple cloning sites between the Nde I and Not I restriction sites was used as initial template (pNH14K) for mutagenesis (Cameron, 2002). Double mutants were generated using the QuickChange site-directed mutagenesis kit (Stratagene) following the manufacturer's guidelines (Figure 2.1a). Mutagenic oligonucleotide primers containing specified point mutations and new restrictions sites (in bold and underlined, respectively) are shown below.

5'-CTTTTGATGAA**C**TCAGGATCGGCATTG-3' (βF55L)

5'-GATTGGGGATGAAGGC**CGG**TGATGAACTCAGGATCG-3' (βF52GβF55L.)

Only the forward primers are shown in each case; the reverse primers were the reverse complement of the sequences shown. The following cycling parameters were used for PCR reactions:

95° C for 30 seconds 1 cycle

95° C for 30 seconds
55° C for 1 minute 12 Cycles
68° C for 12 minutes

The presence of the appropriate mutations was identified by restriction endonuclease digestion and confirmed by DNA sequencing.

The Phusion (Finnzymes) site-directed mutagenesis kit was used to design the single mutant αY122G. The manufacturer's guidelines were followed (Figure 2.1b). The primers used during the PCR reaction are shown below.

Y122G: 5'- Pho - ACT TTA TGT TCA TGTGGC CCT TGG CCA TTG CTT

R122124G: 5'-Pho - GCA GAC TAC AAC ATT GTG TAC CGT ATC CGT A

The following cycling parameters was used:

Initial denaturation	98 °C 30 s	1 cycle
Denaturation	98 °C 10 s	25 cycles
Annealing & Extension	72 °C 5 min	
Final extension	72 °C 10 min	1 cycle

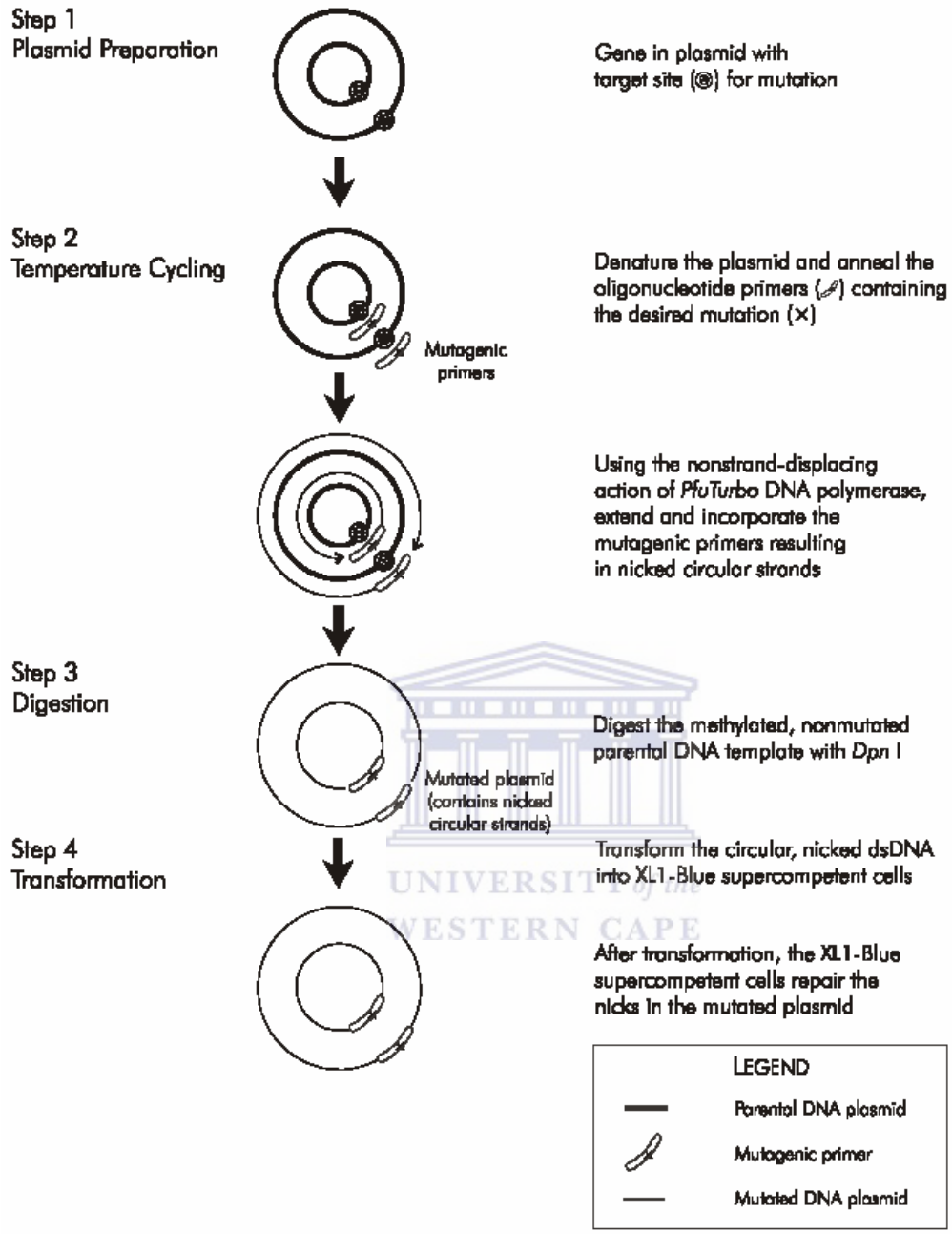

Figure 2.1a: Schematic representation of the Quick-change mutagenesis procedure

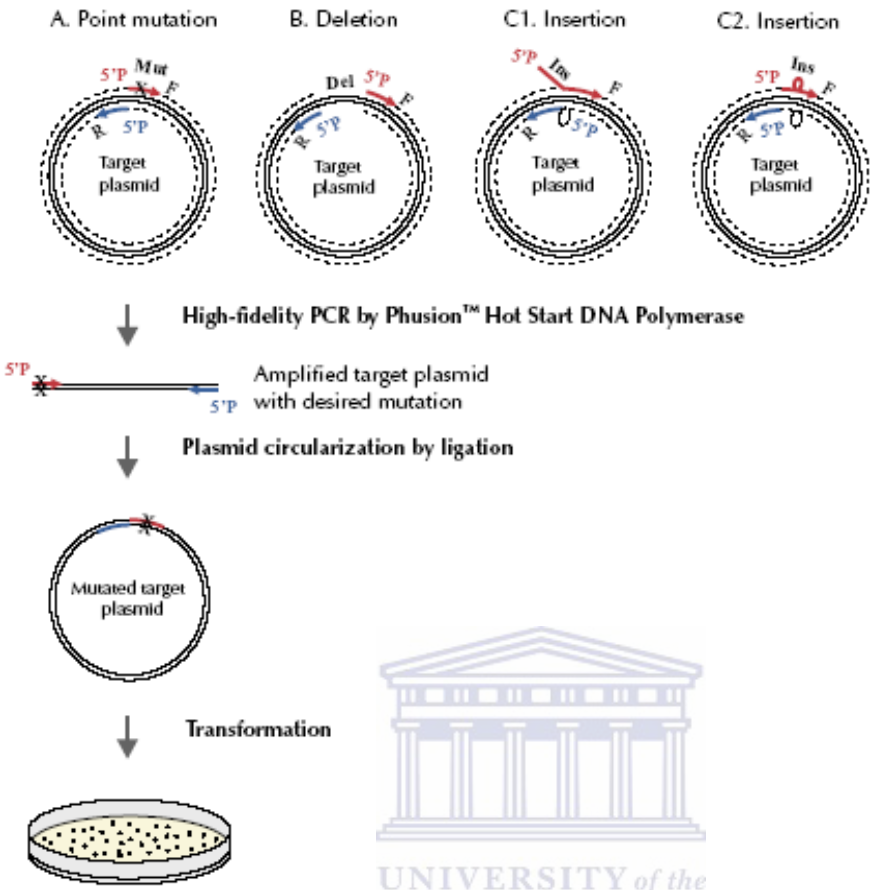

Figure 2.1b: Schematic representation of the Phusion mutagenesis protocol

2.7 Protein expression

Expression of both the wild type and mutant NHases were carried out in *E. coli* BL21 (DE3). Cells were grown at 37 ° C in 500 ml volume of Luria-Bertani (LB) broth containing 70-µg/ml ampicillin. When the optical density (600nm) reached 0.4, cells were induced by the addition of 0.4 mM isopropyl thio-β-D-galactoside (IPTG). 15 to 30 minutes prior to induction cobalt chloride was added to a final concentration of 0.1 mM. Five hours after induction, cells were harvested by centrifugation and washed with 50 mM potassium phosphate buffer pH 7.2. The washed cell pellets were

resuspended in potassium phosphate buffer pH 7.2 and disrupted by one cycle of freezing at -80 ° C and thawing at 37 ° C followed by brief sonication on ice. The cell lysate was centrifuged at 5000 x g and the supernatant precipitated by addition of solid ammonium sulphate to 20 % saturation and incubation on ice for one hour. The suspension was centrifuged at 7000 x g for 30 minutes at 4 ° C to remove the precipitated proteins.

2.8 Protein Purifications

2.8.1 Hydrophobic Interaction chromatography

Clarified supernatant fractions were loaded onto a HighLoad 16/10 Phenyl-Sepharose column pre-equilibrated with 1 M ammonium sulphate in 50 mM potassium phosphate buffer, pH 7.2. A linear gradient of decreasing ammonium sulphate concentration (1M-0M) in 50 mM potassium phosphate buffer pH 7.2 was used to elute the bound proteins

2.8.2 Ion Exchange chromatography

Pooled fractions from Hydrophobic Interaction chromatography were dialysed against 25 mM potassium phosphate buffer, pH 7.2 using Vivaspin 15R 5000 spin filters. Ultrafiltered fractions were loaded onto a HighLoad 26/10 Q-Sepharose FF column, equilibrated with the same buffer. A linear gradient of increasing sodium chloride concentration (0mM-500mM) in 25 mM potassium phosphate buffer, pH 7.2 was used to elute bound proteins.

2.9 Cavity calculations and Normal mode analysis

Unless otherwise stated, all macromolecular structures were visualised using PyMOL (Delano). Site-directed models were prepared by using the mutagenesis tool on PyMOL.

CASTp (http://cast.engr.uic.edu/cgi-bin/cast) was used to compute pocket and cavity volumes. Cavities were visualised using Chime (Elsevier MDL). A probe radius of 1.4 Å (the server default radius) was used for all cavity calculations. The reliability of the results was confirmed with Q-SiteFinder program, which defines a pocket by calculating the van der Waals interaction energies of a methyl probe.

Normal mode analysis of all structures was performed using the Web-server for Normal Mode Analysis of proteins –v2.0 (Hollup *et al*., 2005) together with the ***elNémo*** program, a web interface to the Elastic Network Model (Suhre *et al*., 2004). The web server can be freely accessed at (http://igs-server.cnrs-mrs.fr/elnemo/index.html)

Chapter 3: Engineering and purification of *Geobacillus pallidus* RAPc8 NHase mutants

3.1 Background

As outlined in Section 1.3.3, it has been claimed that cobalt-containing NHases show high levels of substrate specificity (k_{cat}/K_M) on aromatic substrates (Kobayashi and Shimuzu, 1998). However, this hypothesis was later disproved with the characterization of the cobalt type enzymes of *Bacillus smithii* (Tagashima *et al*., 1998), *Bacillus pallidus* DAC 521 (Cowan *et al*, 1998) and (*Geo)Bacillus pallidus* RAPc8 (Pereira *et al*., 1998) that do not show any activity on aromatic nitriles.

Geobacillus pallidus RAPc8 is a thermophilic nitrile degrading isolate, obtained from thermal sediment samples and enriched on solid media containing acetonitrile or propionitrile as the sole nitrogen source (Pereira *et al*., 1998). The optimum growth temperature and constitutive production of nitrile-degrading activity was 60 ºC. Phylogenetic analysis first classified the organism as a *Bacillus* species with 99.9 % 16S rDNA sequence similarity with *Bacillus* sp. (starch negative) (DSM 2349). However, the organism was renamed to *G. pallidus* RAPc8 after the *Bacillus* taxonomy was revised.

Both the native and recombinant *G. pallidus* RAPc8 NHase demonstrated activity on branched, linear and cyclic heteroaromatic nitrile substrates. No detectable activity was found on aromatic nitrile substrates, despite the fact that heteroaromatic nitriles (the cyanopyrimidines) could be catalysed at high k_{cat} values (Pereira *et al*., 1998).

Similar substrate specificity profiles have also been reported for other thermophilic Co-dependent NHases (Hourai *et al*., 2003).

Aromatic products derived from NHase biotransformation play significant roles in the pharmaceutical industries. Benzamide, an important class of anti-inflammatory compounds is commonly used for the treatment of pain, fever and inflammation (naproxen and ibuprofen are commercially important examples). Chemical pathways involved in benzamide synthesis are normally associated with high cost and side chain contaminants (Effenberger and Bohme, 1994; Hann *et al*., 1999). A NHase with high substrate specificity (k_{cat}/K_M) on aromatic nitriles would thus be highly desirable.

Several hypotheses have been presented to explain the lack of activity of the *G. pallidus* NHase on homoaromatic nitriles. The initial hypothesis was that the narrow substrate channel of the enzyme could not accommodate the bulky aromatic ring of the substrate (Nakasako *et al*., 1999). However, this hypothesis was later rejected with the observation that *G. pallidus* NHase showed activity on heteroaromatics (3-cyanopyridine) and yet was unable to hydrate homoaromatics (benzonitrile). It was suggested that, since these substrates are superficially equal in size, *G. pallidus* NHase substrate specificity could not be a function of a small substrate-binding cavity (Cameron, 2002).

It has been reported that benzonitrile acts as a competitive inhibitor of *G. pallidus* NHase activity. It has also been proposed that interactions between the π-clouds of the aromatic substrates and aromatic amino acid residues lining the substrate channel could prevent access of bulky aromatic substrate to the deeply embedded

active site metal ion (Cameron, 2002). Recent studies have revealed that substitution of a tryptophan residue by glycine in helix 5 of the β subunit (βW76G) considerably reduced benzonitrile-induced inhibition compared to the wild type NHase. While the βW76G mutant did not show activity on benzonitrile, analysis of cavities within the crystal structure of the mutant showed an 11% increase in volume and a 20% increase in inner surface area of the substrate channel (Tsekoa, 2005).

In this chapter, attempts to genetically engineer homoaromatic substrate specificity into *G. pallidus* RAPc8 NHase are described.

3.2 Experimental strategy

The apparent inhibition constant (k_i) of benzonitrile on the wild-type RAPc8 NHase was reported as 2.25 mM (Cameron, 2002). Several mutants were constructed by site-specific mutagenesis and benzonitrile inhibition constants determined (Table 3.1). At this stage, enzyme substrate specificity and changes in k_i values could not be directly interpreted. However, based on the non-competitive nature of the inhibition kinetics and the predominance of hydrophobic residues in the vicinity of the active site as shown by X-ray crystallography (Tsekoa, 2005), conformational processes might be implicated in access of substrate (and inhibitor) to the catalytic centre. It can as well be suggested that changes in conformation upon substrate binding might result in a binding site for benzonitrile being exposed. A decrease in k_i on removal of a hydrophobic residue might thus be interpreted as enhanced accessibility to an enzyme-substrate complex in the vicinity of the catalytic site. Conversely, a hydrophobic amino acid deletion mutant resulting in an increase in k_i for benzonitrile

might be interpreted in terms of reduced conformational mobility. Following this hypothesis, mutant βF52G was selected for a further round of mutagenesis.

Table 3.1: Estimated benzonitrile inhibition constants for *G. pallidus* NHase mutants

Mutant	k_i (Benzonitrile) mM
Wild type	2.25
βF36L	2.5
βF52G	0.5
βY67A	3.85
βY67E	8.75
βW76G	31.5

In this attempt to engineer homoaromatic substrate specificity into *G. pallidus* RAPc8 NHase, aromatic amino acids were identified in the proximity of the metal binding site and substituted by site directed mutagenesis with small aliphatic residues (either glycine or leucine). Phenylalanine 55 in the β subunit was thus targeted within the substrate channel. A Model of a F→L mutation showed an increase of 10 % in cavity dimensions when compared to the wild-type. Phenylalanine 55 was substituted with the non-aromatic hydrophobic residue leucine, not only to increase the substrate-binding cavity but also to reduce regional hydrophobicity.

Tyrosine 122 on the α subunit is also among the aromatic amino acids residues proximal to the active site. Due to its apparent proximity to the active site Cobalt atom, and position in the active site channel, tyrosine 122 was also substituted. The

benzonitrile inhibition constant was then determined on the mutant αY122G (data shown in Chapter 4). A low k_i value within the same range to that reported on βF52G (0.5mM) will further support the overall hypothesis.

3.3 Results

3.3.1 Site-directed mutagenesis

The selected aromatic residues were then replaced. In mutagenesis studies aimed at altering specificity or activity, it is preferable to use replacement residues, which do not affect the 3-dimensional fold or stability of the enzyme. Guidelines for the generation of 'safe' substitutions, which are unlikely to distort the protein structure, have been reported (Bordo and Argos, 1991). The preferred substitutions for the aromatic residues are generally other non-polar aliphatic residues. In this study, either G or L was used as a replacement amino acid, thereby reducing both side chain volume and hydrophobicity

The mutations were introduced by means of either the Quick-change (Stratagene) or Phusion (Finnzymes) site-directed mutagenesis kit as described in Section 2.6. Both systems follow a PCR-based approach enabling the mutagenesis to be performed directly on the double-stranded expression construct (βF52G or pNH14K). All the mutations were subsequently verified by DNA sequencing.

3.3.2 Expression and purification of mutants NHase

Expression and purification of the *G. pallidus* RAPc8 NHase mutants was carried out as previously described (Tsekoa, 2004). Expressed NHase was analysed on a 12% SDS PAGE gel (Figure 3.2) and activity on acrylonitrile was verified using the ammonia detection assay. As the wild-type and mutants NHases generated similar expression profile, only the SDS-PAGE gels of the αY122G mutant are shown here.

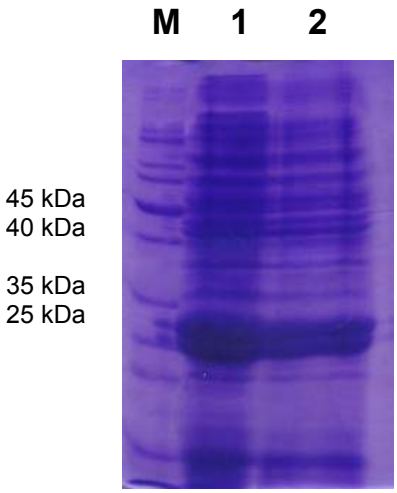

Figure 3.2: SDS-PAGE showing ammonium sulphate treatment. Lane M: molecular weight marker; Lane 1: Crude cell extract; Lane 2: 1 M Ammonium sulphate precipitant.

Both mutants' specific activities were within the same range as that of the wild-type (Table 3.2). Mutant αY122G and βF52GβF55L showed specific activity of 1292 and 1507 U/mg respectively, on the crude cell extract (Table 3.3 and 3.4). Due to the removal of hydrophobic residues, which could have affected the thermostability of the enzymes, none of the mutants were subjected to the heat treatment step. Prior to phenyl-sepharose HIC, the crude extract was treated with 25% w/v saturation of ammonium sulphate. However, because the high concentration of ammonium sulphate interferes with SDS-PAGE and the ammonia assay for NHase activity, it was difficult to quantitatively assess the extent of this purification.

Table 3.2: Purification table for wild-type nitrile hydratase

Step	Volume (ml)	Total Protein (mg)	NHase Activity (Units/ml)	NHase Total Activity (Units)	NHase Specific Activity (Units/mg)	Yield (%)	Purification fold
Crude cell extract	25	200	9480	237000	1185	100	1
Heat treatment	23	117	10870	250000	2136	105	1.8
Phenyl-Sepharose	14	18	11004	154050	8530	65	7.1
Q-Sepharose	10	14	14457	144570	10326	61	8.7

Table 3.3: Purification table for αY122G mutant NHase

Step	Volume (ml)	Total Protein (mg)	NHase Activity (Units/ml)	NHase Total Activity (Units)	NHase Specific Activity (Units/mg)	Yield (%)	Purification fold
Crude cell extract	25	175	9041	226025	1292	100	1
Phenyl-Sepharose	16	25	11754	188064	6028	83	4.7
Q-Sepharose	12	16	14325	171900	7162	71	5.5

Table 3.4: Purification table for βF52GβF55L mutant NHase

Step	Volume (ml)	Total Protein (mg)	NHase Activity (Units/ml)	NHase Total Activity (Units)	NHase Specific Activity (Units/mg)	Yield (%)	Purification fold
Crude cell extract	25	183	11034	275850	1507	100	1
Phenyl-Sepharose	15	23	13221	198315	8641	72	5.7
Q-Sepharose	13	15	15007	195091	13050	70	8.7

Proteins loaded onto the HiLoad 16/10 Phenyl sepharose HP column were eluted at approximately 0.7-0.6 M ammonium sulphate. The resulting chromatogram is shown in Figure 3.3. Fractions from peak M (on the chromatogram) were analysed by SDS-PAGE (Figure 3.4). Pooled fractions were assayed for NHase activity. This step resulted in 83% and 72% of NHase activity for the αY122G and βF52GβF55L mutant respectively.

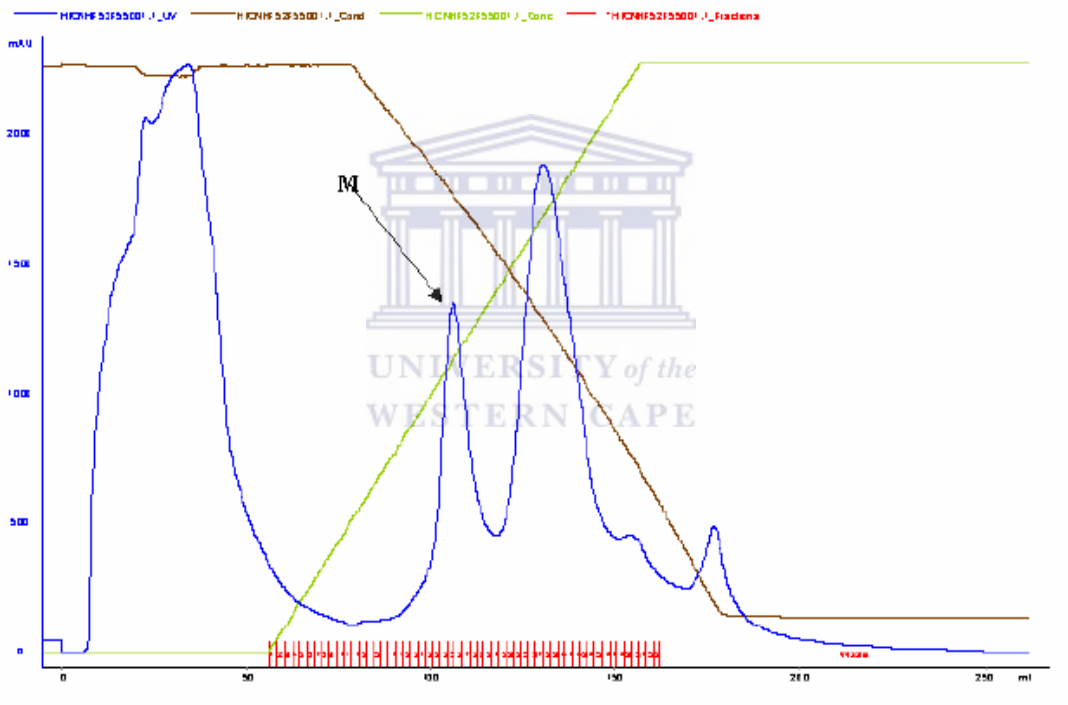

Figure 3.3: Chromatogram of Phenyl-Sepharose Hydrophobic Interactions**.** M: Peak corresponding to putative NHase. The yellow line indicates the % Buffer B (0-100), the blue line indicates relative conductivity.

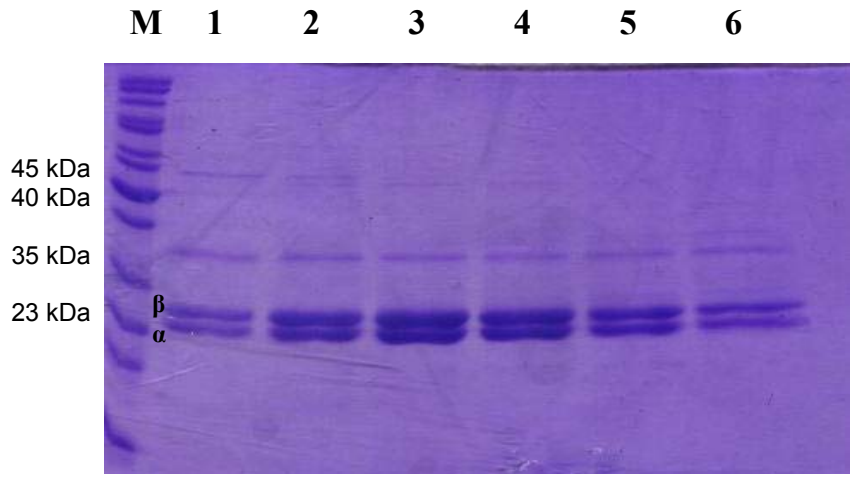

Figure 3.4: SDS-PAGE gel showing HIC treatment. Lane M: molecular weight marker; Lane 1-6: HIC fractions

The dialysed factions from HIC were purified using anion exchange chromatography. Bound proteins were eluted with a 5 column-volume linear gradient at approximately 185-240 mM sodium chloride. Fractions were analysed by SDS-PAGE (Figure 3.6). The chromatogram is illustrated in Figure 3.5. Assay for NHase on the pooled fractions revealed around 70% yield for both αY122G and βF52GβF55L mutant.

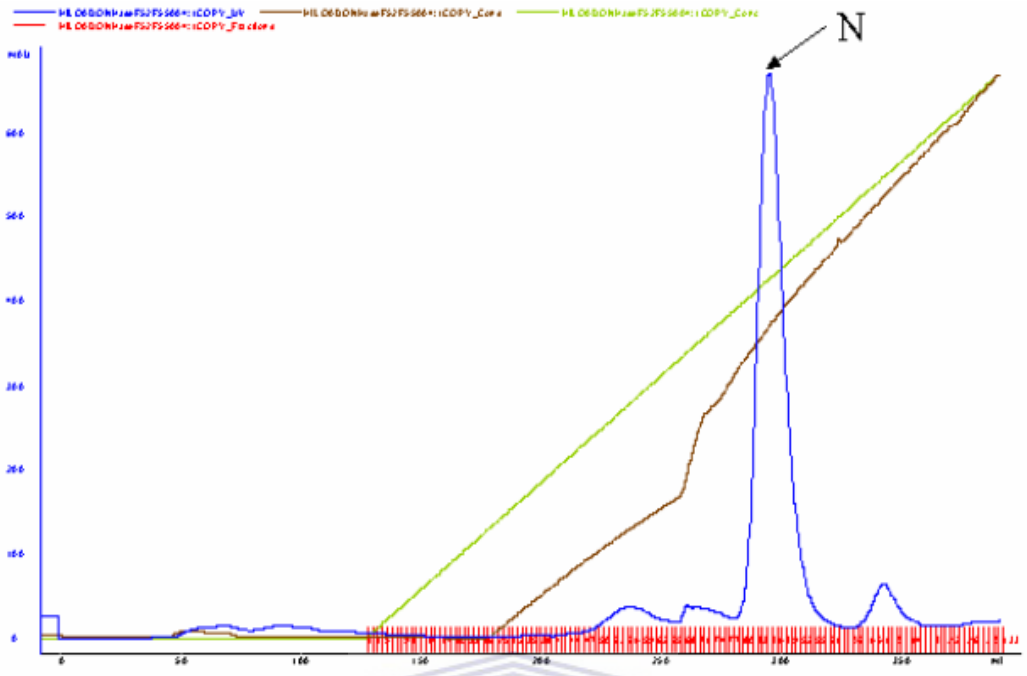

Figure 3.5: Chromatogram of Q-sepharose Ion Exchange. N: Peak corresponding to putative NHase. The yellow line indicates the % Buffer B (0-100), the blue line indicates relative conductivity.

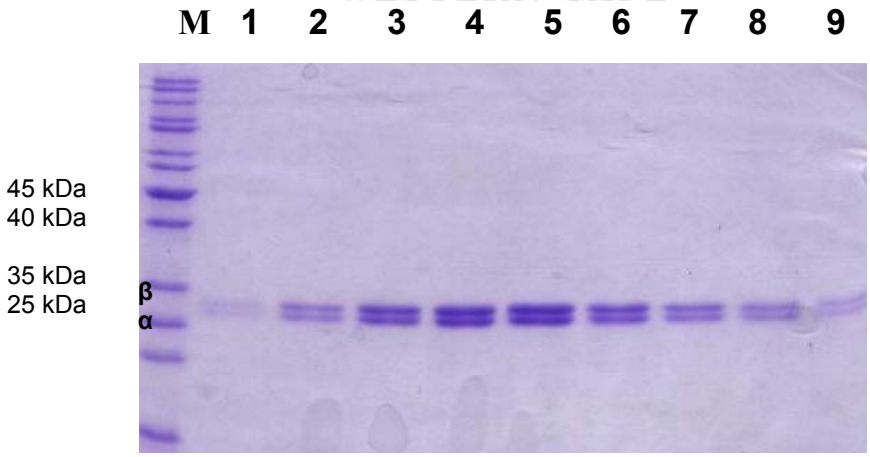

Figure 3.6: SDS-PAGE gel showing IE treatment. Lane M: molecular weight marker; Lane 1-9: IC fractions

Chapter 4: Kinetic data and cavity calculations

4.1 Background

In a previous study (Cameron, 2002) a discontinuous assay was used for the characterization of a range of *G. pallidus* RAPc8 mutants. The limitations of such an assay in kinetic analysis may include timing and volume inaccuracies associated with the withdrawal of samples at fixed times (Cornish-Bowden, 1995). In addition, the shape of the progress curve during the reaction is not readily apparent (Atkins and Nimmo, 1975). Thus it is important to verify that the estimated rates generated in such assays are truly proportional to the enzyme concentration. In this study, a different approach, as described in Section 2.5.5, was used.

Experimental investigations of enzymes are preferentially performed using homogeneous protein samples. This is because the use of crude cell extracts or semi-pure proteins might complicate the analysis due to the presence of multiple activities, side reactions or intrinsic inhibitors. In earlier studies (Cameron, 2002) attempting to engineer homoaromatic substrate specificity into *G. pallidus* RAPc8 NHase, well-defined protocols for generating pure enzyme was not yet available. However, a purification protocol developed by Tsekoa (2006) made it possible to generate high yields of homogeneous NHase for subsequent kinetic analyses.

The presence of upstream and/or downstream open reading frames has been shown to be important for expression of many NHases in an active form. Overproduction of *P. putida* NHase requires co-expression of a P14K gene, found immediately downstream of the NHase β subunit (Cameron *et al*., 2005; Wu, 1997). Similar

proteins found downstream of the NHase genes of *Bacillus* sp. BR449 and *R. rhodochrous* J1 (Kim and Oriel, 2000; Komeda, 1996a, 1996b) were also necessary for efficient NHase production.

4.2 Kinetic data of βF52GβF55L mutant

Standard kinetics for the conversion of acrylonitrile and benzonitrile were determined on the mutant βF52GβF55L using a continuous assay. The formation of each product was measured at an absorbance of 225 and 242 nm, respectively. The outputs obtained from the straight-line transformation curve of the Michaelis-Menten equation are shown in Table 4.1a and 4.1b. The data were analysed using the Lineweaver-Burke, Hanes, Eadie-Hofstee, the direct linear and the non-linear regression of the Wilkinson method. However for easy visualisation, these data are shown here using an Eadie-Hofstee plot (Figure 4.1). The limitations and merits of each method of calculation have previously been discussed (Eisenthal and Cornish-Bowden, 1974). The values obtained from the Direct-Linear plot were considered as the most reliable. Statistical analysis of the kinetic data for the double mutant is shown in Table 4.2.

Table 4.1a: Kinetic constants of wild-type *G. pallidus* RAPc8 NHase on acrylonitrile and benzonitrile substrates

Substrates		Lineweaver-Burke	Hanes	Eadie-Hofstee	Direct Linear	Wilkinson
Acrylonitrile	K_M (mM)	9.71	10.2	9.53	11.5	11.0
	V_{max} (U/mg)	1400	1624	1529	1300	1326
Benzonitrile	K_M (mM)	-	-	-	-	-
	V_{max} (U/mg)	-	-	-	-	-

Table 4.1b: Kinetic constants of *G. pallidus* RAPc8 NHase double mutant on acrylonitrile and benzonitrile substrates

Substrates		**Lineweaver-Burke**	**Hanes**	**Eadie-Hofstee**	**Direct Linear**	**Wilkinson**
Acrylonitrile	K_M (mM)	1.70	3.09	1.99	2.58	3.37
	V_{max} (U/mg)	435	738	641	730	752
Benzonitrile	K_M (mM)	0.347	0.145	0.136	0.305	0.117
	V_{max} (U/mg)	1189	1084	977	1100	1143

A

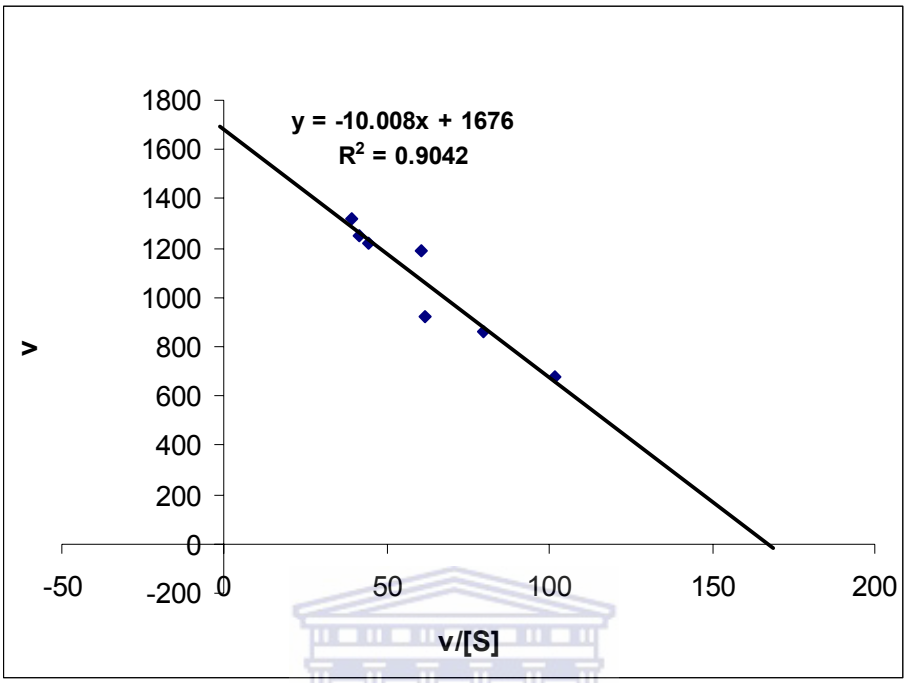

B

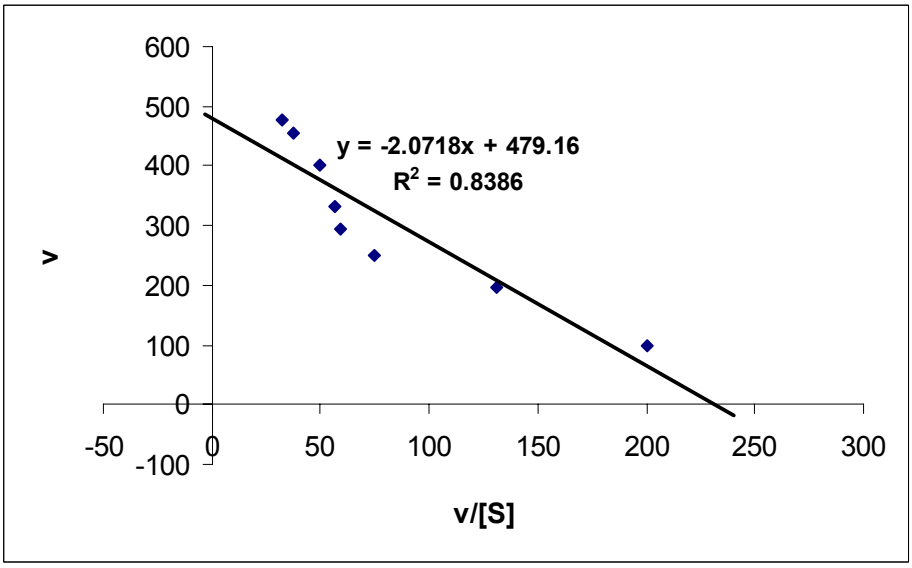

C

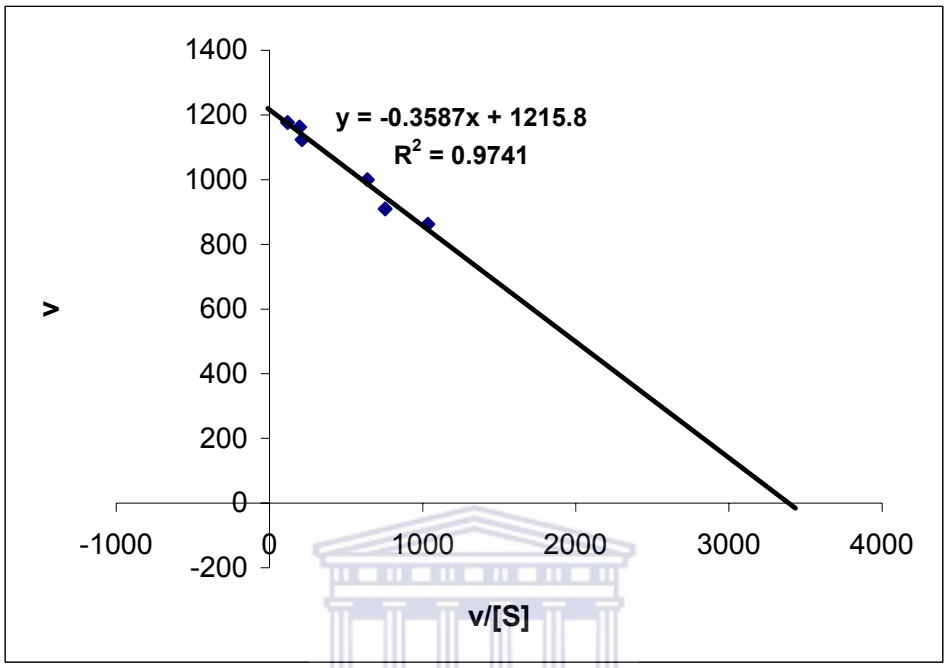

Figure 4.1: Eadie-Hofstee plot of kinetic data of: A wild-type NHase on acrylonitrile; B double mutant NHase on acrylonitrile; C double mutant NHase on benzonitrile

The substrate binding affinity of the wild-type *G. pallidus* RAPc8 NHase for acrylonitrile was consistent with previously reported data (Cameron, 2002; Tsekoa, 2005). The determined K_M was also within the same range displayed by the native enzyme (11mM) (Pereira, 1998a). The observed variations in V_{max} could be accounted for in terms of the different methods used for NHase characterization in each study. Whilst the use of semi-pure enzyme in the kinetic assay is unlikely to have a direct effect on the K_M values, a significant change in V_{max} would be expected on comparison to the use of fully purified enzyme. The K_M determined in this study also compares well with that observed for various mesophilic NHase: R. rhodochrous

J1 H-NHase (11.8 mM) (Nagasawa, 1991), R. rhodochrous J1 L-NHase (11.9 mM) (Wieser, 1998). No apparent activity was detected on benzonitrile with the wild type NHase.

Table 4.2a: Kinetic constants of wild type NHase on acrylonitrile and benzonitrile as calculated using the direct linear plot analysis

Substrates	K_M (mM)	68% confidence limits	V_{max} (U/mg)	68% confidence limits	k_{cat} (s^{-1})	k_{cat}/K_M ($s^{-1}.mM^{-1}$)
Acrylonitrile	11.5	9.57-14.1	1300	1247-1463	1995 - 2340	141-245
Benzonitrile	-	-	-	-	-	-

Table 4.2b: Kinetic constants of βF55LβF52G NHase on acrylonitrile and benzonitrile as calculated using the direct linear plot analysis

Substrates	K_M (mM)	68% confidence limits	V_{max} (U/mg)	68% confidence limits	k_{cat} (s^{-1})	k_{cat}/K_M ($s^{-1}.mM^{-1}$)
Acrylonitrile	2.6	2.04-3.12	730	676-760	1082-1216	347-596
Benzonitrile	0.3	0.19-0.42	1100	988-1192	1581-1907	4540-8321

The high k_{cat}/K_M value of the double mutant suggests that changes in the substrate channel and conformation of the enzyme may be two possible interactive mechanisms for homoaromatic recognition at the catalytic site. βF52 and βF55 residues are proposed here to be the most critical residues serving as inhibitor-binding sites in the wild-type RAPc8 NHase. From a mechanical point of view, both phenylalanine residues could serve as targets for interfering with the dynamics of the

enzyme (Yang and Bahar, 2005). As a result, they prevent efficient recognition of homoaromatic substrates and minimization of intermolecular interactions at the catalytic site cleft. The calculated k_{cat} of the double mutant for benzonitrile conversion is of the same order as in the catalysis of acrylonitrile by the wild type enzyme. Kinetic analyses also suggest that the double mutant has a high level of aromatic specificity given that the specificity constant (k_{cat}/K_M) is about 12 fold higher than that for acrylonitrile. The k_{cat}/K_M calculated for the *G. pallidus* NHase double mutant on benzonitrile is comparable with that of the cobalt-type *Pseudonocardia thermophilia* JCM 3095 NHase (6150 $s^{-1}.mM^{-1}$) (Hourai *et al*., 2003).

Therefore, these results provide evidence concerning the role of the two-phenylalanine residues (βF55βF52) at the catalytic centre. CASTp analysis shows that atoms CD2, CE2 and CZ of Phe52 and atoms CD1, CE1 and CZ of Phe55 contributed directly to the lining of the substrate channel. It was proposed that these residues are involved in the stabilisation of the active site cleft by aromatic-aromatic interactions in *Bacillus smithii* NHase (Hourai *et al*., 2003). The observed change in substrate specificity also suggests that conformational changes may be implicated for trapping homoaromatic substrate in a catalytic orientation. The K_M of acrylonitrile is also noted to be approximately 4-fold lower in the double mutant compared to the wild-type enzyme, suggesting that the binding strength of the substrate at the catalytic centre has greatly enhanced.

4.3 Enzyme kinetic inhibition of αY122G mutant

In the wild-type structure of RAPc8 NHase, amino acid residue αY122 is 10.69 Å from the cobalt atom. The location of this residue within the substrate channel can clearly be seen (Figure 4.2). According to CASTp analysis, this residue directly contributes to the lining of the substrate channel.

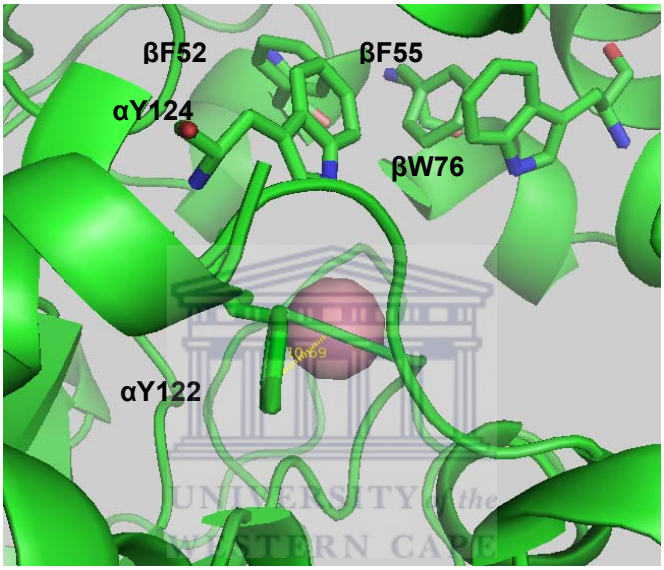

Figure 4.2: The location of residue αY122 at the catalytic centre of the wild-type *G. pallidus* RAPc8 NHase

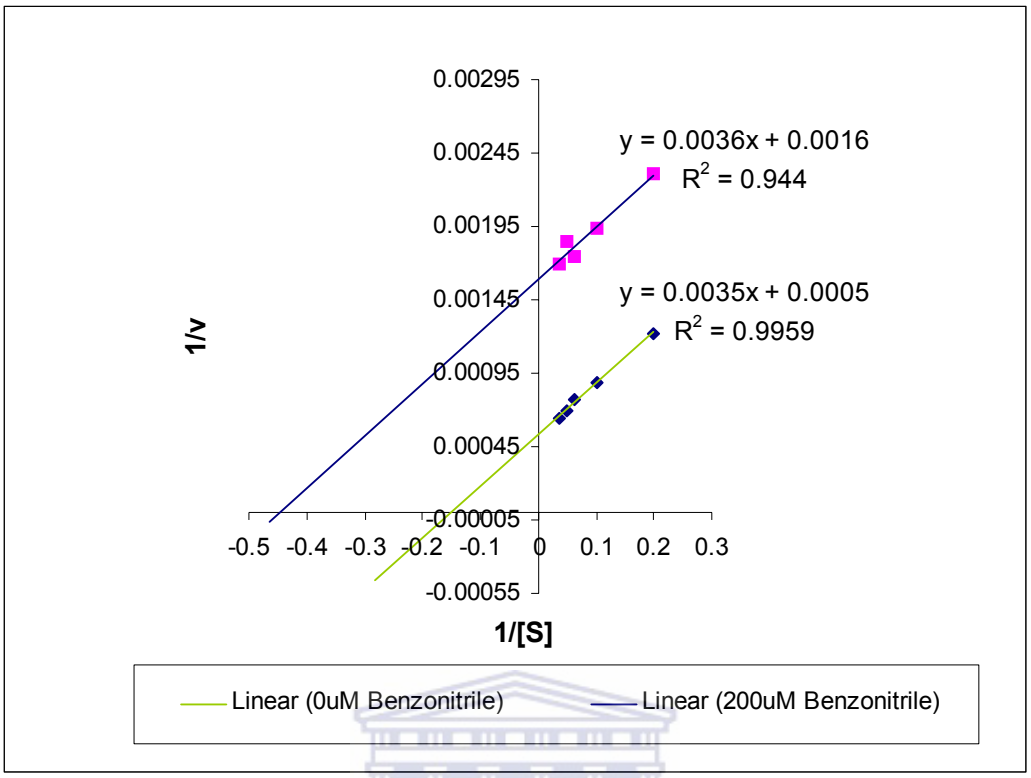

Figure 4.3: Lineweaver-Burke plot of αY122G mutant NHase in the presence and absence of benzonitrile using acrylonitrile as substrate

The Y→G mutation at position 122 on the α-subunit did not result in detectable levels of activity on benzonitrile. However, the mutation resulted in an increase in inhibition of about 20 fold. The data are presented using a Lineweaver-Burke plot (Figure 4.3). The calculated Kinetic data are shown in Table 4.3. The data in the presence of 200 μM of benzonitrile show a significant change in both V_{max} and K_M. The V_{max} to K_M ratio was constant in the presence and absence of inhibitor. These observed changes in V_{max} and K_M together with a constant V_{max}/K_M are characteristic of uncompetitive inhibition. It can therefore be hypothesised that on binding of the substrate to the enzyme, a conformational change occurs, which presents a binding site for benzonitrile. The apparent inhibition constant was found to be 120 μM.

Comparison of the low K_i of the αY122 mutant with the K_M for acrylonitrile indicates that the strength of inhibition by benzonitrile was very high.

Table 4.3: Kinetic constants of αY122G mutant NHase in the presence and absence of benzonitrile using acrylonitrile as substrate

[Benzonitrile] (μM)	K_M (mM)	V_{max} (U/mg)	V_{max}/K_M
0	5.8	1748	301
200	2.10	630	300

4.4 Cavity calculations

The crystal structure of the wild-type *G. pallidus* RAPc8 NHase was recently determined at a resolution of 2.5 Å (Tsekoa, 2005). The static structure together with additional computational programs gives rich insights about the binding of biologically functional ligands around the active site, leading to catalysis. In this Section, analysis of the catalytic cavities of the wild-type *G. pallidus* RAPc8 NHase and the double mutant model are described and compared.

Structural analysis of the molecular surface was carried out and visualized in PyMOL (DeLano Scientific). All water molecules were purposefully removed (dry state) so that the surface observed is that contributed by the amino acid residues only. Site-directed mutant model was prepared as described in Section 2.9. Assessment of the wild-type molecular surface identified a continuous channel with possible access to the bulk solvent from two locations in the heterodimer (Figure 4.4). The channel goes across the metal centre that is located in the central cavity formed at the interface

between the α and β subunits. At this stage there were no major differences observed between the wild-type structure and the double mutant model.

Cavity calculations on the wild-type and double mutant NHase were done using the CASTp server (Liang *et al*., 1998). A probe radius of 1.5 Á was used for the initial search of pockets/cavities. The program identified a total of 74 pockets for the wild-type and 73 pockets for the double mutant. However, only those that intrude deep enough to the catalytic centre (Co^{3+}) of the protein were chosen for further analysis. All the amino acid residues that contribute to the lining of the channel are listed in Table 4.4.

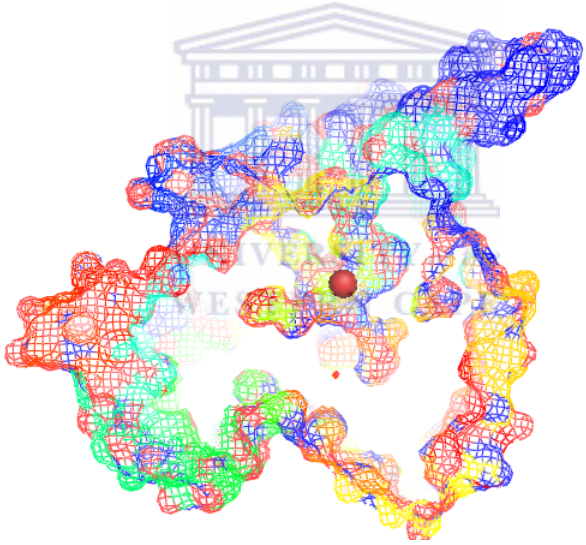

Figure 4.4: Mesh representation of molecular surface in the dry state to illustrate internal cavities. A continuous channel transversing the metal binding site (red sphere) can be seen.

Table 4.4: Amino acid residues that line the substrate channel in the wild-type RAPc8 NHase

Pocket	α-subunit	β-subunit
1	Gln88, Leu109, Ser121, Tyr122, Trp127, Leu129, Pro130, Lys135, Glu136, Pro137, Arg140	His5, Phe36, Phe52, Phe55, Arg56, Ile59, Glu60, Tyr67, Leu68, Thr69, Ser71, Tyr72, Tyr73, His75, Trp76, Arg166
2	Leu87, Glu90, Ser161, Ser162, Glu163	Lys50, Ala51, Asp53, Glu54, Lys130, Pro132, Arg134, His158, His179, Val180, Pro182, Ala185, Arg188, Gly190, Glu191, Trp220

The two largest pockets identified by CASTp are described here as pocket 1 and 2 respectively. Unlike what has been described earlier on in this Section, pocket 1 and 2 form two distinct curved extended channels in the wild-type heterodimer (Figure 4.5a). Analysis of cavity dimensions shows clearly that the substrate channel for the wild-type NHase in each dimer is not continuous. The cavity leading to the active centre is lined with aromatic residues (βPhe52, βPhe55, βPhe36, βTyr67, βTrp76, αY122 and αW124G). Among all these residues αW124G is strongly conserved whereas βPhe52 and βPhe36 are the least conserved among all known NHases.

In the double mutant model, CASTp identifies a single channel transversing the αβ dimer with opposing openings (Figure 4.5b). The continuous channel has no amino acid at the centre blocking the passage of any substrate, which could gain access to the catalytic site from either side of the mouth openings. A comparison of the

substrate channel showed an increase of 29 % in cavity volume and 13 % in internal surface area for the βF52LβF55G mutant over the wild-type NHase (Table 4.5).

A

B

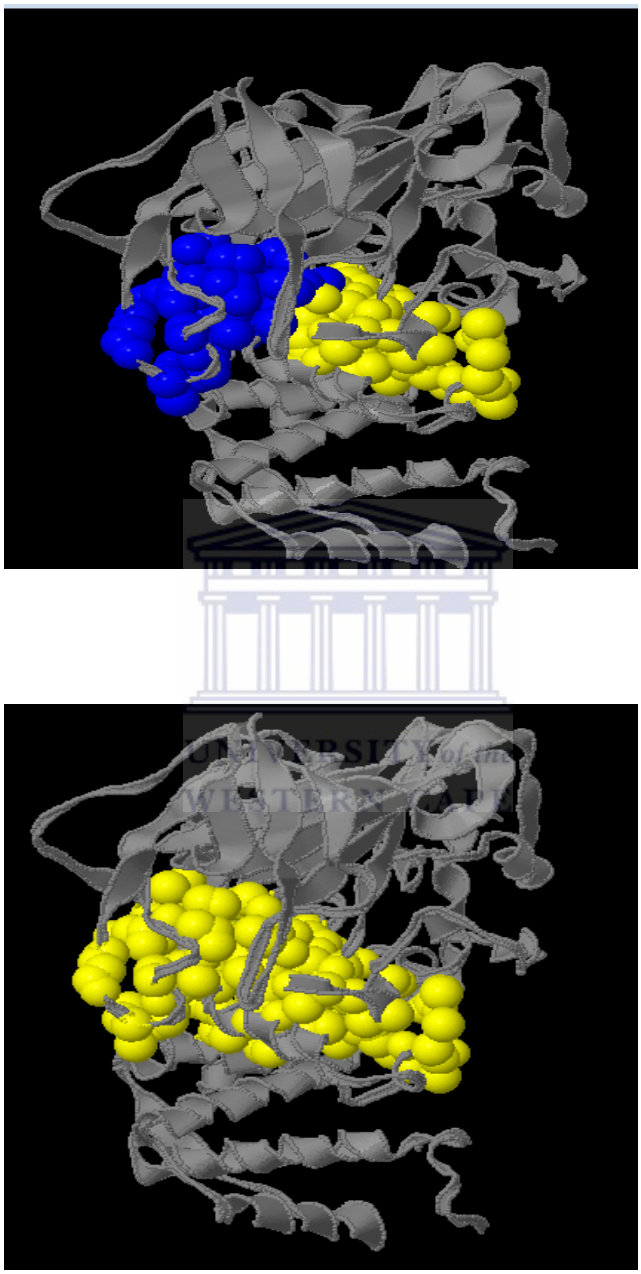

Figure 4.5: (A) Two major pockets/cavities within the wild-type *G. pallidus* RAPc8 NHase identified using a probe radius of 1.5 Å. These pockets overlap with each other to form an extended channel that transverses the cobalt centre. (B) One single continuous pocket transversing the cobalt centre within the double mutant NHase. (Figure generated using CASTp (Liang *et al*., 2006) and Chime)

Table 4.5: Geometric dimensions of the substrate channel for the wild-type and mutant NHase calculated by CASTp on the heterodimer

	Cavity	Volume (Å^3)	Inner surface area (Å^2)
Wild-type	1	580.6	588.2
	2	497.1	474.3
Mutant	1	1400	1200

Bacillus smithii NHase, which also exhibits higher substrate specificity (k_{cat}/K_M) for aliphatic nitriles over aromatic substrates, contains βPhe52 at the catalytic centre (Hourai *et al*., 2003). It was proposed that the Phe52 in the β subunit of *B. smithii* NHase covers the metal centre partially like a 'rigid lid' thus narrowing the active site cleft. Using the same approach, based on an increase in cavity dimensions (removal of the F52 lid) together with the existence of a single channel per dimer, access of homoaromatic substrates is greatly enhanced to the catalytic site of the double mutant. The un-competitive inhibition of benzonitrile (Tsekoa, 2005) to the RAPc8 NHase now suggests that both the substrate (acrylonitrile) and inhibitor (benzonitrile) presumably gain access to the enzyme through the same substrate channel. The non-hydrophobic nature of the substrate together with its small size facilitates its catalysis at the metal centre, while the inhibitor forms strong aromatic-aromatic interactions (explain by the low k_i showed in Table 3.1) with F52 and F55 on the β subunit. The inhibitor only affects the enzyme-substrate complex resulting in a lower K_M and V_{max} (data not shown) during substrate conversion.

4.5 Normal Mode Analysis

The intrinsic flexibility of the wild-type and double mutant NHase was assessed using the Normal Mode Analysis (NMA) calculations. NMA identifies potential conformational changes based on vibrational modes of atoms in a molecule (Hollup *et al*., 2005). The program interprets changes in vibrational modes in terms of deformation energy. Low deformation energy relates to a highly rigid domain whereas a high value defines higher degree of intrinsic flexibility. The deformation energies of about 200 lowest frequency modes were computed by NMA.

The deformation energy of the double mutant was slightly higher than that of the wild-type NHase (Table 4.6). The difference of 10 units may indicate a slightly higher degree of conformational flexibility at localised positions in the double mutant, which might probably be absent in the wild-type.

Table 4.6: The lowest deformation energies of the least frequency modes of NHase

NHase structure	Deformation energy (J/mol)
β55Lβ52G	565.9
Geobacillus pallidus RAPc8	575.7

As explained above, the removal of the F52 and F55 on the β subunit might have resulted in a possible decrease in π-π interactions between the aromatic rings of the substrate and the aromatic residues lining the substrate channel. The decrease in aromatic interactions has possibly allowed the bulky homoaromatic substrate to

reach the catalytic site. In addition, the slight increase in intrinsic movements could have induced functionally relevant homoaromatic substrate recognition in the double mutant NHase. Therefore, the kinetic constants data together with the slight increase in intrinsic flexibility for the double mutant are completely consistent with our mechanistic model; conformational processes are implicated in substrate access to the active site.

Conformational changes create movements that may be described as shear motion in protein structures. Shear motions are parallel to the interface between the closely packed segments of the protein. These motions induce changes in the main and side chain torsion angles of the segments in the protein interface (Perutz, 1983; Gerstein *et al*., 1994). The various movements of each segment as oppose to one another gives rise to 'flip-flop' substrate entry mechanism. In the double mutant NHase, a similar mechanism could be used to explain the possible entrance of substrate into the active site channel. Alternation in segments between the C-terminals of the β subunits and N-terminals of the α-subunits generated by shear motions controls the access of substrate into the four possible entrances of the mutant enzyme (Figure 4.4). 'Flip-flop' entry mechanism and shear motions might not be directly related to catalysis but may contribute towards homoaromatic substrate recognition in the mutant (Bishop and Sewell, 2006).

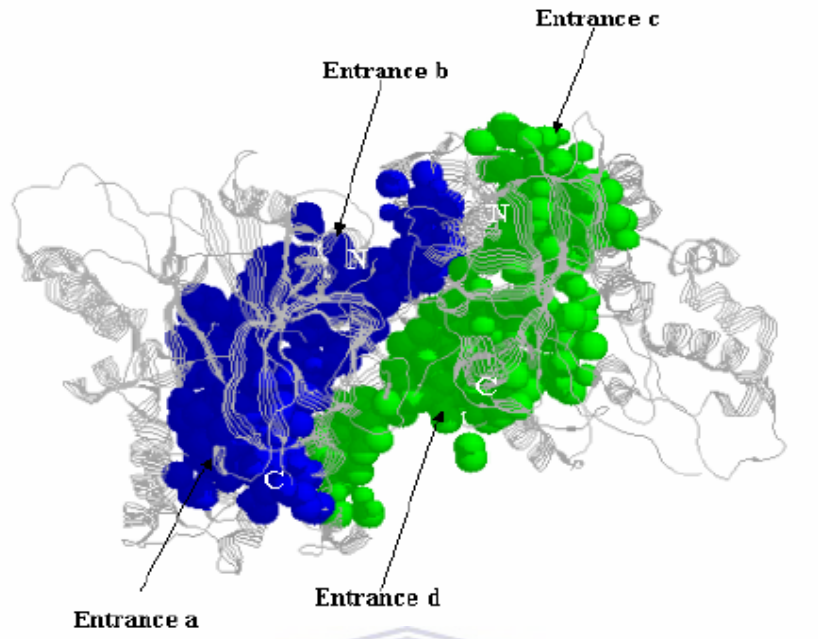

Figure 4.6: Cavities within the double mutant NHase. Shear motions cause segments around the C-terminals of the β subunits to come closer to each other, with the simultaneous moving apart of segments around the N-terminals of the α subunits or vice versa. Substrate may enter through entrance b, when the N-terminal segments of the α move apart or enter through channel d when the C-terminal segments of the β moves apart.

Chapter 5: General Discussion

The primary objective of the work presented in this thesis was to engineer homoaromatic substrate-specificity into *G. pallidus* RAPc8 NHase. This was accomplished using a rational design approach, where site-specific mutations were used to substitute aromatic residues within the substrate channel. The double mutant βF52LβF55G was successfully designed, expressed and purified to homogeneity.

To date, this is the third report aiming at engineering aromatic substrate specificity into RAPc8 NHase. Despite consecutive failures on the first two attempts (Cameron, 2002; Tsekoa, 2005), their reported results contributed largely towards the successful designing of this work. In a previous hypothesis, the lack of homoaromatic activity in the RAPc8 NHase was assumed to be a function of both substrate channel volume and π-π cloud interactions between the aromatic substrates and aromatic residues lining the enzymatic cavity. It was reported that RAPc8 NHase degrades 3-cyanopyridine with high k_{cat} value but yet fails to catalyse benzonitrile (Pereira *et al*., 1998). Based on this observation, it was suggested that a narrow entrance to the active site could not alone be responsible towards lack of homoaromatic specificity in the RAPc8 NHase. A change in the enzyme conformation was thus assumed to be crucial for homoaromatic substrate recognition (Lesk and Chotia, 1984; Gutteridge and Thornton, 2005).

It was further reported that benzonitrile acts as a competitive inhibitor with a calculated k_i of 2.25 mM on the wild-type enzyme. Several site-directed mutants were made and their k_i values were subsequently analysed. βF52G resulted with the lowest k_i value (0.5 mM) (Cameron, 2002). The F→G mutation has increased side

chain flexibility at this localised position given that glycine possess the least limited rotational freedom at the N-C^{α} bond (Huang and Nau, 2003). Since side chain flexibility and conformation are highly related in protein structures (Carugo and Argos, 1997), substitutions of the more constrained phenylalanine to the highly flexible glycine mediated access of benzonitrile to the catalytic centre. A decrease in k_i was thus interpreted as enhanced accessibility as well as enhanced conformational mobility to an inhibitor-binding site in the vicinity of the active centre. βF52G was therefore selected for further mutagenesis.

The determination of the molecular structure of the RAPc8 NHase (Tsekoa, 2005) facilitated the analysis of the residues lining the substrate channel. In the attempt to further increase the substrate channel volume, βF55 was targeted due to its close proximity to the Co^{3+} ion of the cavity-binding site. The F→L mutation on the β subunit did not only result to an increase in cavity volume but contributed towards a reduction in regional hydrophobicity. Phe 55 is separated by 4.78 Å from Phe 52. Two residues would be considered to be interacting if they are positioned within a range of 4 Å apart (Gunasekaran and Nussinov, 2006). Thus, the simultaneous removal of the two phenylalanine residues was expected to decrease the larger rotational barrier imposed by the bulky aromatic rings that impeded benzonitrile access to the catalytic centre.

Enzyme kinetic studies were performed using a continuous spectrophotometric assay. The kinetic parameters of the wild-type and mutant protein on acrylonitrile and benzonitrile as substrates were analysed and compared. The double mutant demonstrated activity on benzonitrile, with a calculated k_{cat} value comparable with the

catalysis of acrylonitrile by the wild-type enzyme. Besides having a high turnover number, kinetic analysis also revealed a high level of aromatic specificity in the double mutant given that the specificity constant (k_{cat}/K_M) was about 12 fold higher than that of acrylonitrile. At this stage, comparisons of estimated kinetic constants (K_M and k_{cat}) indicate that the double mutant can compete with the catalyst *Pseudonocardia thermophilia* NHase (Miyanaga *et al*., 2004) in terms of efficiency for commercial production of benzamide. Drawing on the data generated, this finding indicated a likely role for residues βF55 and βF52 as an inhibitor-binding site in the wild-type RAPc8 NHase.

Comparison in cavity dimensions showed an increase of 29 % in volume and 13 % in surface area for the double mutant to that of the wild-type enzyme. Based on this structural information, it could be speculated that since βF52 partially covers the Co^{3+} ion like a 'rigid lid' in the wild-type enzyme, the active site cleft is significantly narrowed, thus preventing access of the bulky aromatic substrates to the catalytic centre. Therefore, it can be concluded that Phe 52 on the β subunit plays a key role for the substrate specificity of this enzyme. The removal of the F52 has contributed to the presence of a continuous channel transversing the entire length of each dimer for the mutant enzyme. The presence of a single channel, together with four possible entrances for substrates may have enhanced homoaromatic substrates recognition in the F52GF55L mutant.

Conformational dynamics has recently been recognised as a mechanism supporting catalytic activity (Luo and Bruice, 2004; Ringe and Petsko, 2004). Changes in enzyme conformation are normally classified in terms of either domain or loop motion

(Kempner, 1993). However in the absence of an experimentally solved structure for the double mutant, prediction on the type of conformational change is not possible at this stage. Thus, a different approach was used to compare the inherent flexibility of the double mutant with the wild-type RAPc8 NHase. Normal mode analysis showed a marginal increase in intrinsic flexibility for the double mutant over the wild-type enzyme. The increase in flexibility may have induced functionally relevant conformation in the mutant NHase, facilitating the access of the bulky homoaromatic substrates towards the catalytic site. Changes in conformation, may have also favoured the preferential binding of the homoaromatic substrate in a catalytic orientation.

K_M and V_{max} were determined for the αY122G mutant. Although this mutation did not result in activity on benzonitrile, the strength of inhibition was several fold higher than that of the wild-type. This finding indicated a likely role for residue αY122 in benzonitrile binding. The observed changes in V_{max} and K_M were an indication that the type of inhibition was un-competitive. Based on these data and following the working hypothesis presented in this work, the designing of a triple mutant βF52LβF55GαY122G could further improve substrate specificity on benzonitrile.

Based on the actual findings of this work, a plausible mechanistic model for benzonitrile substrate specificity may be defined in terms of both hydrophobicity (interactions between aromatic substrates and aromatic residues within the substrate channel) and protein conformational mobility.

References

Asano, Y., Tani, Y., and Yamada, H. (1980) A new enzyme 'nitrile hydratase' which degrades acetonitrile in combination with amidase. *Agricultural and Biological Chemistry*. **44:** 2251-2252.

Asano, Y., Fujishiro, K., Tani, Y., and Yamada, H. (1982) Aliphatic nitrile hydratase *arthrobacter* sp. J-1. Purification and characterization. *Agricultural and Biological Chemistry*. **46:** 1165-117.

Artaud, I., Chatel, S., Chauvin, A. S., Bonnet, D., Kopf, M. A., and Leduc, P. (1999) Nitrile hydratase and related non-heme iron sulfur complexes. *Coodination Chemistry Reviews*.**190:** 577-586.

Atkins, G. L., and Nimmo, I. A. (1975) A comparison of seven methods for fitting the Michaelis-Menten equation. *Biochemical Journal*. **149:** 775-7.

Battistel, E., Bernandi, A., and Maestri, P. (1997) Enzymatic decontamination of aqueous polymer emulsions containing acrylonitrile. *Biotechnology Letters*. **19:** 131-134.

Bigey, F., Chebrou, H., Fournand, D., and Arnaud, A. (1999). Transcriptional analysis of the nitrile-degrading operon from *Rhodococcus* sp. Acv2 and high

level production of recombinant amidase with an *Escherichia coli* -T7 expression system. *Journal of Applied Microbiology*. **86:** 752-760.

Bishop, A. O. T., and Sewell, B. T. (2006) A new possible approach to possible substrate binding mechanisms for nitrile hydratase. *Biochemical and Biophysical Research Communications*. **343:** 319-325.

Bordo, D., and Argos, P. (1991) Suggestions for safe residue substitutions in site-directed mutagenesis. *Journal of Molecular Biology*. **4:** 721-729

Bradford, M. M. (1976) A rapid and sensitive method for the quantitation of microgram quantities of protein utilizing the principle of protein-dye binding. *Analytical Biochemistry.* **72:** 248-54.

Cameron, R. A., Sayed, M. F., and Cowan, D. A. (2005) Molecular analysis of the nitrile catabolism operon of the thermophile *Bacillus pallidus* RAPc8. *Biochimica Biophysica Acta.* **1725:** 35-46.

Cameron, R. A. (2002) Nitrile degrading enzymes from extreme environments. *Ph.D. thesis*, University of London, London, UK.

Carugo, O., and Argos, P. (1997) Correlation between side chain mobility and conformation in protein structures. *Protein Engineering.* **10:** 777-787.

Cornish-Bowden, A. (1995) Fundamentals of enzyme kinetics. Portland Press, London, UK.

Cowan, D. A., Meyer, Q., Stafford, W., Muyanga, S., Cameron, R. A., and Wittwer, P. (2005) Metagenomics gene discovery: past, present and future. *Trends in biotechnology*. **23:** 321-329.

Cowan, D. A., Cameron, R. A., and Tsekoa, T. L. (2003) Comparative biology of mesophilic and thermophilic nitrile hydratases. *Advances in applied microbiology*. **52:** 123-153.

Cowan, D. A., Cramp, R. A., Pereira, R., Graham, D., and Almatawah, Q. (1998) Biochemistry and biotechnology of mesophilic and thermophilic nitrile metabolizing enzymes. *Extremophiles.* **2:** 207-216.

Cramp, R. A. and Cowan, D. A. (1999) Molecular characterisation of a novel thermophilic nitrile hydratase. *Biochimica et Biophysica Acta (BBA) - Protein Structure and Molecular Enzymology.* **1431:** 249-260.

Cunningham, K. I., Northup, D. E., Pollastro, R. M., Wright, W. E., LaRock, E. J. (1995) Bacteria, Fungi and Biokarst in Legchuguilla cave, Carlsbad caverns National Park, New Mexico. *Environmental Geology*. **25:** 2-8.

Duran, R., Nishiyama, M., Horinouchi, S. and Beppu, T. (1993) Characterization of nitrile hydratase genes cloned by DNA screening from *Rhodococcus erythropolis*. *Bioscience Biotechnology and Biochemistry*. **57:** 1323-8.

Effenberger, F. and Bohme, J. (1994) Enzyme-catalysed enantioselective hydrolysis of racemic naproxen nitrile. *Bioorganic and Medicinal Chemistry*. **2:** 715-21.

Eisenthal, I. R., and Cornish-Bowden, A. (1974) The direct linear plot. A new graphical procedure for estimating enzyme kinetic parameters. *Biochemical Journal*. **139:** 715-20.

Endo, I., Nojiri, M., Tsujimura, M., Nakasako, M., Nagashima, S., Yohda, M., and Odaka, M. (2001) Fe-type nitrile hydratase. *Journal of Inorganic Biochemistry.* **83:** 247-253.

Endo, I., and Odaka. M. (2000) What evidences were elucidated about photoreactive nitrile hydratase? *Journal of Molecular Catalysis B: Enzymatic*. **10:** 81-86.

Endo, I., Odaka, M., and Yohda, M. (1999) An enzyme controlled by light: the molecular mechanism of photoreactivity in nitrile hydratase. *Trends in Biotechnology*. **17:** 244-248.

Fallon, R. D., Stieglitz, B., and Turner, I. (1997) A *Pseudomonas pudita* capable of stereoselective hydrolysis of nitriles. *Applied Microbiology Biotechnology.* **47:** 156-161.

Fawcett, J., and Scott, J. (1960) A rapid and precise method for the determination of urea. *Journal of Clinical Pathology*. **13:** 156-159.

Gunasekaran, K., and Nussinov, R. (2006) How different are structurally flexible and rigid binding sites? Sequences and structural features discriminating proteins that do and do not undergo conformational change upon ligand binding. *Journal of Molecular Biology.* **365:** 257-273.

Gutteridge, A., and Thornton, J. (2005) Conformational changes observed in enzyme crystal structures upon substrate binding. *Journal of Molecular Biology*. **346:** 21-8.

Hann, E. C., Eisenberg, A., Fager, S. K., Perkins, N. E., Gallagher, F. G., Cooper, S. M., Gavagan, J. E., Stieglitz, B., Hennessey, S. M. and DiCosimo,

R. (1999) 5-Cyanovaleramide production using immobilized *Pseudomonas chlororaphis* B23. *Bioorganic and Medicinal Chemistry*. **7:** 2239-45.

Hashimoto, Y., Sasaki, S., Herai, S., Oinuma, K., Shimizu, S., and Kobayashi, M. (2002) Site-directed mutagenesis for cysteine residues of cobalt-containing nitrile hydratase. *Journal of Inorganic Biochemistry*. **91:** 70-77.

Heald, S. C., Brandao, P. F., Hardicre, R., and Bull, A. T. (2001) Physiology, Biochemistry and taxonomy of deep-sea nitrile metabolizing Rhodococcus strains. *Antonie Van Leeuwenhoek*. **80:** 169-183.

Heveling, J., Armbruster, E., Utiger, L., Rohner, M., Dettwiler, H., and Chuck, R. (1998) Process for preparing nicotinamide. U.S. patent 5,719,045.

Hollup, S. M., Salensminde, G., and Reuter, N. (2005) WEBnm@: a web application for normal mode analysis of proteins. BMC Bioinf. **6:** 52.

Hourai, S., Miki, M., Takashima, Y., Mitsuda, S. and Yanagi, K. (2003) Crystal structure of nitrile hydratase from a thermophilic *Bacillus smithii*. *Biochemical and Biophysical Research Communications.* **312:** 340-5.

Huang, F., and Nau, W. M. (2003) A conformational flexibility scale for amino acids in peptides. *Angewandte Chemie.* **42:** 2262-2272.

Huang, W., Jia, J., Cummings, J., Nelson, M., Schneider, G., and Lindqvist, Y. (1997) Crystal structure of nitrile hydratase reveals a novel iron centre in a novel fold. *Structure.* **5:** 691-699.

Iketha, O., Nishiyama, M., Horinouchi, S., Beppu, T. (1989) Primary structure of nitrile hydratase deduced from the nucleotide sequence of a *Rhodococcus* species and its expression in *Escherichia coli*. *European Journal of Biochemistry*. **181:** 563-570.

Kato, Y., Ooi, R., and Asano, Y. (1998) Isolation and characterization of a bacterium possessing a novel aldoxime-dehydration activity and nitrile-degrading enzymes. *Archives of Microbiology.* **170:** 85-90.

Kato, Y., Yoshida, S., Xie, S. X., and Asano, Y. (2004) Aldoxime dehydratase coexisting with nitrile hydratase and amidase in the iron-type nitrile hydratase-producer *Rhodococcus* sp N-771. *Journal of Bioscience and Bioengineering.* **97:** 250-259.

Kempner, E. S. (1993) Movable lobes and flexible loops in proteins. Structural deformations that control biochemical activity. *FEBS Letters.* **326:** 4-10.

Kim, S., and Oriel, P. (2000) Cloning and expression of the nitrile hydratase and

amidase genes from *Bacillus* sp. BR449 into *Escherichia coli*. *Enzyme and Microbial Technology*. **27:** 492-501.

Kobayashi, M., and Shimuzu, S. (1998) Metalloenzyme nitrile hydratase: Structure, regulation, and application to biotechnology. *Nature Biotechnology*. **16:** 733-736.

Kobayashi, M., Nagasawa, T., and Yamada, H. (1992) Enzymatic synthesis of acrylamide: a success story not yet over. *Trends in Biotechnology.* **10:** 402-408.

Komeda, H., Kobayashi, M., and Shimuzu, S. (1996a) A novel gene cluster including the *Rhodococcus rhodochrous* J1 nhlba genes encoding a low molecular mass nitrile hydratase (L-NHase) induced by its reaction product. *Journal of Biological Chemistry.* **271:** 15796-15802.

Komeda, H., Kobayashi, M., and Shimuzu, S. (1996b) Characterization of the gene-cluster of high-molecular-mass nitrile hydratase (H-NHase) induced by its reaction-product in *Rhodococcus rhodochrous* J1. *Proceedings of the National Academy of Sciences*, *USA*. **93:** 4267-4272.

Kwofie, S. (2006) Crystal structure of a mutant NHase*. MSc thesis*, University of Cape Town, RSA.

Legras, J., Chuzel, A., Arnaud, A., and Galzy, P. (1990) Natural nitriles and their metabolism. *World Journal Microbiology Biotechnology*. **6:** 83-108.

Lesk, A., and Chotia, C. (1984) Mechanisms of domain closure on proteins. *Journal of Molecular Biology*. **174:** 175-191.

Liang, J., Edelsbrunner, H., and Woodward, C. (1998) Anatomy of Protein Pockets and Cavities: Measurement of Binding Site Geometry and Implications for Ligand Design. *Protein Science*. **7:** 1884-1897

Lourenco, P. M., Almeida, T., Mendonca, D., Simoes, F., and Novo, C. (2004) Searching for nitrile hydratase using the Consensus-Degenerate Hybrid Oligonucleotide Primers strategy. *Journal of Basic Microbiology*. **44:** 203-14.

Lu, J., Zheng, Y., Yamagishi, H., Odaka, M., Tsujimura, M., Maeda, M., and Endo, I. (2003) Motif CXCC in nitrile hydratase activator is critical for NHase biogenesis in vivo. *Federation of European Biochemical Societies-Letters*. **553:** 391-396.

Luo, J., and Bruice, T. C. (2004) Anticorrelated motions as a driving force in enzyme catalysis: the dehydrogenase reaction. *Procedings of the National Academy of Science,* USA. **101:** 13152-13156.

Mascharak, P. (2002) Structural and functional models of nitrile hydratase. *Coordination Chemistry Reviews*. **225:** 201-214.

Miyanaga, A., Fushinobu, S., Ito, K., Shoun, H. and Wakagi, T. (2004) Mutational and structural analysis of cobalt-containing nitrile hydratase on substrate and metal binding. *European Journal of Biochemistry*. **271:** 429-38.

Miyanaga, A., Fushinobu, S., Ito K., and Wakagi, T. (2001) Crystal structure of cobaltcontaining nitrile hydratase. *Biochemical and Biophysical Research Communications.* **288:** 1169-74.

Mylerova, V., and Martinokova, L. (2003) Synthetic applications of nitrile-converting enzymes. *Current Organic Chemistry.* **7:** 1-17.

Nagasawa, T., and Yamada, H. (1995) Interrelations of chemistry and biotechnology. 6. Microbial production of commodity chemicals. *Pure Applied Chemistry*. **67:** 1241-1256.

Nagasawa, T., and Yamada, H. (1989) Microbial transformations of nitriles. *Trends in Biotechnology*. **7:** 153-158.

Nagasawa, T., Ryuno, K., and Yamada, H. (1986) Nitrile hydratase of *Brevibacterium* R312-purification and characterization. *Biochemical Biophysical Research Communications*. **139:** 1305-1309.

Nagashima, S., Nakasako, M., Dohmae, N., Tsujimura, M., Takio, K., Odaka, M., Yohda, M., Kamiya, N., and Endo, I. (1998) Novel non-heme iron centre of nitrile hydratase with a claw setting of oxygen atoms. *Nature Structural Biology.* **5:** 347-351.

Nakasako, M., Odaka, M., Yohda, M., Dohmae, N., Takio, K., Kamiya, N., and Endo I. (1999) Tertiary and quaternary structures of photoreactive Fe-type nitrile hydratase from Rhodococcus sp. N771: Roles of hydration water molecules in stabilizing the structures and the structural origin of the substrate specificity of the enzyme. *Biochemistry.* **3:** 9887-9898.

Nelson, M. J., Jin, H. Y., Turner, I. M., Grove, G., Scarrow, R. C., Brennan, B. A., and Que, L. (1991) Cloning and characterization of genes responsible for metabolism of nitrile compounds from Pseudomonas chlororaphis B23. *Journal of Bacteriology.* **173:** 2465-2472.

Noguchi, T., Honda, J., Nagamune, T., Sasabe, H., Inoue, Y., and Endo, I. (1995) Photosensitive nitrile hydratase intrinsically possesses nitric oxide bound

to the nonheme iron centrer: evidence by Fourier transform infrared spectroscopy. *FEBS Letters*. **358:** 9-12.

Pace, N. R. (1997) A molecular view of microbial diversity and the bioshere. *Science*. **276:** 734-740

Padmakumar, R. and Oriel, P. (1999) Bioconversion of acrylonitrile to acrylamide using a thermostable nitrile hydratase. *Applied Biochemistry and Biotechnology.* **77-9:** 671-679.

Pereira, R. A., Graham, D., Rainey, F. A., and Cowan, D. A. (1998) A novel thermostable nitrile hydratase. *Extremophiles.* **2:** 347-357.

.**Precigou, S., Goulas, P., and Duran, R.** (2001) Rapid and specific identification of nitrile hydratase (NHase)-encoding genes in soil samples by polymerase chain reaction. *FEMS Microbiology Letters.* **204:** 155-161.

Ringe, D., and Petsko, G. A. (2004) The 'glass' transition in protein dynamics: what it is, why it occurs, and how to exploit it. Biophysical Chemistry. **105:** 667-680.

Sambrook, J., and Russell, D. W. (2001) Molecular cloning: A laboratory manual. Cold Spring Harbor Laboatory Press, New York, USA.

Sari, M. A., Moali, C., Boucher, J. L., Jaoven, M., and Munsuy, D. (1998) Detection of a nitrile oxide synthase possibly involved in the regulation of the *Rhodococcus* sp. R312 nitrile hydratase. *Biochemical and Biophysical Research Communications*. **250:** 364-368.

Schloss, P. D., and Handelsman, J. (2003) Biotechnological prospects from metagenomics. *Current Opinion in Biotechnology*. **14:** 303-310.

Shi, Y., Yu, H., Sun, X., Tian, Z., and Shen, Z. (2004) Cloning of the nitrile hydratase gene from *Nocardia* sp. in *Escherichia coli* and *Pichia pastoris* and its functional expression using site-directed mutagenesis. *Enzyme and Microbial Technology*. **35:** 557-562.

Stalker, D.M., McBride, K.E., and Mahyi, L.D. (1998) Herbicide resistance in transgenic plants expressing a bacterial detoxification gene. *Science*. **242**: 41-423

Stevens, J. M., Rao Saroja, N., Jaouen, M., Belghazi, M., Schmitter, J. M., and Mansuy, D. (2003) Chaperone-assisted expression, purification, and characterization of recombinant nitrile hydratase NI1 from *Comamonas testosteroni*. *Protein Expression and Purification.* **29:** 70-76.

Streit, W. R., and Schimtz, R. A. (2004) Metagenomics-the key to the uncultured microbes. *Current Opinion in Microbiology*. **7:** 492-498.

Suhre, K., and Sanejouand, Y. (2004) ElNemo: a normal mode web server for protein movement analysis and the generation of templates for molecular replacement. *Nucleic acids*. **32:** 610-614.

Takashima, Y., Yamaga, Y., and Mitsuda, S. (1998) Nitrile hydratase from a thermophilic *Bacillus smithii*. *Journal of Industrial Microbiology & Biotechnology.* **20:** 220-226.

Thomas, S. M., DiCosimo, R., and Nagarajan, A. (2002) Biocatalysis: applications and potentials for the chemical industry. *Trends in Biotechnology.* **20:** 238-242.

Tsekoa, T. L. (2005) Structure, enzymology and genetic engineering of *Bacillus* sp. RARc8 Nitrile Hydratase. *Ph.D thesis*, University of the Western Cape, RSA.

Tsekoa, T. L., Sayed, M. F., Cameron, R. A., Sewell, B.T. and Cowan, D.A. (2004) Purification, crystallization and preliminary X-ray diffraction analysis of thermostable nitrile hydratase. *South African Journal of Science.* **100:** 488-490.

Valera, F. R. (2004) Environmental genomics, the big picture? *FEMS Microbiology Letters*. **231:** 153-158.

Wieser, M., Takeuchi, K., Wada, Y., Yamada, H., and Nagasawa, T. (1998) Low molecular-mass nitrile hydratase from *Rhodococcus rhodochrous* J1: Purification, substrate specificity and comparison with the analogous high-molecular-mass enzyme. *FEMS Microbiology Letters*. **169:** 17-22

Wu, S., Fallon R. D., and Payne, M. S. (1997) Over-production of stereoselective nitrile hydratase from *Pseudomonas putida* 5B in *Escherichia coli*: activity requires a novel downstream protein. *Applied Microbiology and Biotechnology.* **48:** 704-708.

Wyatt, J.M and Knowles, C.J. (1995) The development of a novel strategy for the microbial treatment of acrylonitrile effluents. *Biodegradation*. **6:** 93-107.

Yamada, H., and Kobayashi, M. (1996) Nitrile hydratase and its application to industrial production of acrylamide. *Bioscience Biotechnology and Biochemistry*. **60:** 1391-400.

Yamamoto, K., Ueno, Y., Otsubo, K., Yamane, H., Komatsu, K., and Tani, Y. (1992) Efficient conversion of dinitrile to mononitrile-monocarboxylic acid by *Corynebacterium* sp. C5 cells during tranexamic acid synthesis. *Journal of Fermentation and Bioengineering.* **73:** 125-129.

Yang, L. W., and Bahar, I. (2005) Coupling with catalytic site and collective dynamics: A requirement for mechanochemical activity of enzymes. *Structure.* **13:** 893-904.

Zaks, A. (2001) Industrial biocatalysis. *Current Opinion in Chemical Biology.* **5:** 130-136.

Appendices

Appendix 1 ***Biorad protein assay standard curve***

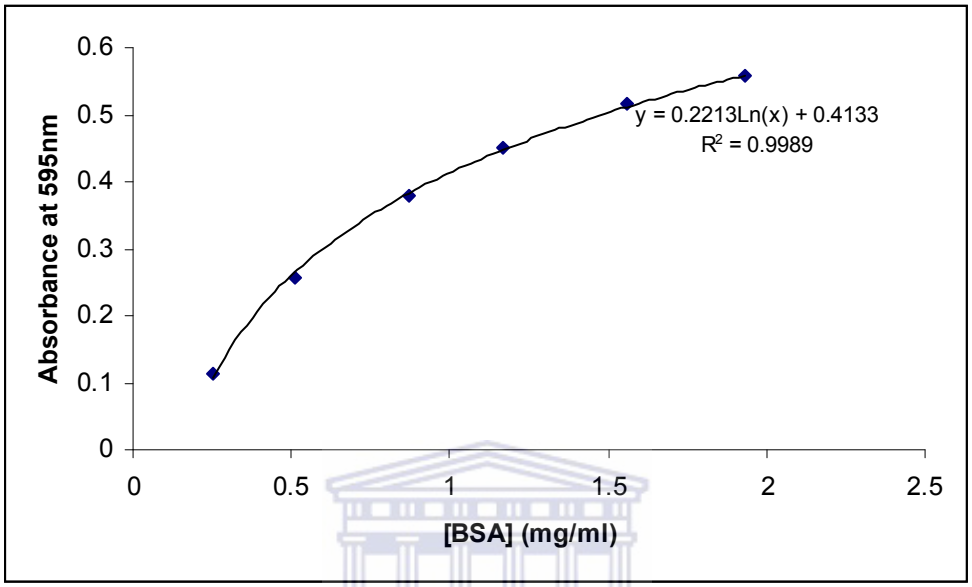

Appendix 2 **Ammonia assay standard curve**

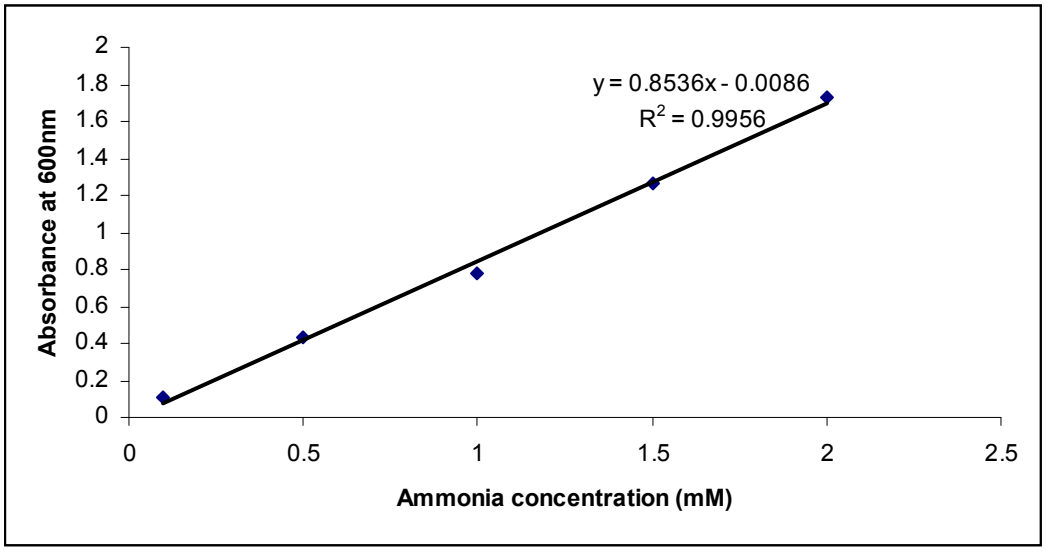

Appendix 3 **Notation used for description of atoms in phenylalanine**